NASA CONTRACTOR REPORT 177456

Concepts for Radically Increasing the Numerical Convergence Rate of the Euler Equations

D. Nixon
K.L. Tzuoo
S.C. Caruso
M. Farshchi
G.H. Klopfer
A. Ayoub

CONTRACT NAS2-12129
May 1987

National Aeronautics and
Space Administration

NASA
National Aeronautics and Space Administration

Report Documentation Page

1. Report No.	2. Government Accession No.	3. Recipient's Catalog No.
NASA CR 177456		

4. Title and Subtitle	5. Report Date
Concepts for Radically Increasing the Numerical Convergence Rate of the Euler Equation	May 1987
	6. Performing Organization Code

7. Author(s)	8. Performing Organization Report No.
David Nixon, Keh-Lih Tzuoo, Steven C. Caruso, Mohammad Farshchi, Goetz H. Klopfer, Alfred Ayoub	
	10. Work Unit No. 505-60-01

9. Performing Organization Name and Address	11. Contract or Grant No.
Nielsen Engineering & Research, Inc. 510 Clyde Avenue Mountain View, CA 94043-2287	NAS2 - 12129
	13. Type of Report and Period Covered

12. Sponsoring Agency Name and Address	
NASA Ames Research Center Moffett Field, CA 94035	Contractor Report
	14. Sponsoring Agency Code

15. Supplementary Notes

Point of Contact: H. Lomax, Ames Research Center, M/S 202A-1, Moffett Field, CA 94035 (415)694-5126 or FTS 464-5126

16. Abstract

Integral equation and finite difference methods have been developed for solving transonic flow problems using linearized forms of the transonic small disturbance and Euler equations. A key element is the use of a strained coordinate system in which the shock remains fixed. Additional criteria are developed to determine the free parameters in the coordinate straining; these free parameters are functions of the shock location. An integral equation analysis showed that the shock is located by ensuring that no expansion shocks exist in the solution. The expansion shock appears as oscillations in the solution near the sonic line, and the correct shock location is determined by removing these oscillations. A second objective was to study the ability of the Euler equations to model separated flow.

17. Key Words (Suggested by Author(s))	18. Distribution Statement
Euler equations, transonic flow, small disturbance equations, finite difference method, integral equation method	Unlimited STAR Category: 02

19. Security Classif. (of this report)	20. Security Classif. (of this page)	21. No. of pages	22. Price
Unclassified	Unclassified	82	

NASA CONTRACTOR REPORT 177456

Concepts for Radically Increasing the Numerical Convergence Rate of the Euler Equations

D. Nixon
K.L. Tzuoo
S.C. Caruso
M. Farshchi
G.H. Klopfer
A. Ayoub

Prepared for
Ames Research Center
under Contract NAS2 - 12129
May 1987

National Aeronautics and
Space Administration

Ames Research Center
Moffett Field, California 94035

COPY NO. 4

CONCEPTS FOR RADICALLY INCREASING THE NUMERICAL CONVERGENCE RATE OF THE EULER EQUATIONS

by

David Nixon,
Keh-Lih Tzuoo, Steven C. Caruso,
Mohammad Farshchi, Goetz H. Klopfer,
and Alfred Ayoub

NEAR TR 380
May 1987

Prepared Under Contract No. NAS2-12129

for

Ames Research Center
National Aeronautics and Space Administration
Moffett Field, CA 94035

NIELSEN ENGINEERING & RESEARCH, INC.
510 Clyde Avenue
Mountain View, California 94043-2287
Telephone: (415)968-9457

TABLE OF CONTENTS

1. Introduction 3

2. A Study of a Discrepancy Noted in Phase I 5

3. Studies of the TSD Equation 7
   3.1 Introduction 7
   3.2 Basic Equations 9
   3.3 Analysis 14
   3.4 Origin of the Oscillatory Behavior 18
   3.5 Multiple Coordinate Straining 22
   3.6 Summary 22
   3.7 Linearized Solutions of the Differential TSD Equation 23

4. Linear Perturbation Equations with Constant Coefficients 25
   4.1 Introduction 25
   4.2 Basic Equations 26
   4.3 Possibility of Deriving a Closed Form Solution ... 30
   4.5 Results 33
5. Perturbation of the Euler Equations 33
   5.1 Introduction 33
   5.2 Basic Equations 33
   5.3 Linearized Euler Equations 36
   5.4 Results 42
   5.5 Concluding Remarks 42

6. Analysis of the Modeling of Separated Flow Using the Euler Equations 42
   6.1 Introduction 42
   6.2 Analysis 43
   6.3 Additional Comments on "Euler" Separation 53

7. Concluding Remarks 57

8. References 59

CONCEPTS FOR RADICALLY INCREASING THE NUMERICAL CONVERGENCE RATE OF THE EULER EQUATIONS

1.) Introduction

There is considerable interest at the present time in solving the Euler equations to predict fluid flow. The Euler equations are assumed to be good approximations of the Reynolds averaged Navier-Stokes equations when modeling attached flows with shock waves and rotational effects as well as being much cheaper to compute because the fine details of the physical viscous region are neglected.

All of the current methods of solving the Euler equations, for example those of Reference 1, rely on iteration procedures that linearize the governing equations about values at the previous iteration level. The impetus behind the present study is to determine a better function or base solution for the linearization in order to reduce the number of iterations and, in particular, to determine whether the number of iterations can be reduced to one.

In Reference 2, which is the report on the Phase I effort, a study of the transonic small disturbance (TSD) equation is described. The idea behind the study of the TSD equation is that it is a simple nonlinear equation which can represent shock waves. If this equation can be linearized so that shock waves can be represented then this technique may be transferable to the Euler equations. In Reference 2 applications of the transonic perturbation technique, developed by Nixon (Ref. 3), are investigated with the conclusion that a linearized solution of the TSD equation is feasible. However, during the course of the study it was found that a solution of the linearized partial differential equation obtained by the integral equation technique differed greatly from solutions obtained by a finite difference technique. Since it is anticipated that general solutions to the linearized Euler and TSD equations will be obtained by finite

difference methods, this is a disturbing result. It is suggested also in Reference 2 that a closed form solution of the TSD equation could be found.

This report is concerned with extensions of the studies given in Reference 2, in particular a more detailed examination of the TSD equation and the extension to the Euler equations. It had been the intention to extend the investigation to include three dimensional flows but lack of time and funds precluded this step. The report is written as a series of relatively self contained sections to facilitate understanding. In Section (2) the anomaly between integral equation and finite difference solutions of the TSD equation reported in Reference 2 is resolved. The conclusion is that the finite difference technique applied a fictitious constraint on the solution thus leading to erroneous results.

Section (3) is concerned mainly with further studies of the integral equation formulation of the TSD equation. One of the more surprising results of the study is that the original formulation of the transonic perturbation method given in References 3 and 4 is incorrect although the published results are correct because of a numerical smoothing in the computations. An important result is that an arbitrary solution of the integral form of the TSD equation, that is a solution that does not locate the shock wave, gives oscillatory behavior in the neighborhood of the sonic line. This oscillatory behavior is a numerical representation of the mathematically derived expansion shock. The correct shock location is that which removes these oscillations, which indicates that the oscillations are a critical consequence of the formulation. A dissipative finite difference solution of the linearized TSD equation removes these oscillations by numerical means and thus removes the necessary information for determining the shock location. A non-dissipative finite difference solution is derived which does locate the shock wave correctly. The results of both integral equation and finite difference results indicate that linearization of the TSD equation can lead to adequate results.

In Section (4) an attempt to use a linearized TSD equation with constant coefficients is described. If sufficiently accurate, this would allow a transonic solution to be constructed using superposition of two Prandtl Glauert solutions, one subsonic and one supersonic. The results of this study are inconclusive; good results can be obtained but the technique seems to be very sensitive to numerical errors.

In Section (5) the techniques developed for the finite difference solution of the TSD equation are applied to the linearized Euler equations. It is found that the odd and even points in the Euler solution have to be decoupled before adequate solutions can be obtained. It is concluded that solutions of the linearized Euler equations can be of adequate accuracy, although it must be stated that this conclusion is based on limited experience.

In Section (6) a study is made of separation phenomena modeled by the Euler equations. It is concluded that although separation can be modeled by the Euler equations, it does not have much in common with real (physical) viscosity controlled separation. It is found also that specifying an empirically determined separation line is not consistent with the Euler equation formulation. Finally, it is suggested the boundary conditions commonly used in numerical solutions of the Euler equations are inconsistent.

2.) A Study of a Discrepancy Noted in Phase I

In the Phase I work two methods of calculating the linearized TSD equation were used, namely an integral equation method and a finite difference method. The TSD equation is linearized about a piecewise constant base flow with one portion giving an elliptic equation and the other a hyperbolic equation. In the finite difference solution, calculated using a modified version of the TSFOIL code (Ref. 5), the solution in the

hyberbolic zone is subsonic, while part of the flow in the elliptic domain is supersonic. This anomalous behavior must be understood before further work is performed since it may be due to inherent difficulties in the finite difference approximation. An example of the anomalous behavior is shown in Figure 1.

The computational code used in these computations is TSFOIL (Ref. 5) which solves the equation

$$(1-u_o)\phi_{xx} + \phi_{yy} = 0 \tag{1}$$

where ϕ is a perturbation velocity potential and $u_o = 0$ or 2; when $u_o = 0$ the equation is elliptic and when $u_o = 2$ the equation is hyperbolic. At the "sonic line" (upstream limit of the hyperbolic domain) the algorithm in TSFOIL puts

$$\phi_{yy} = 0 \tag{2}$$

since in a continuous distribution of u_o, u_o is unity (sonic) at this boundary. However, since u_o is discontinuous in Equation (1), the application of Equation (2) makes

$$\phi_{xx} = \frac{\partial u}{\partial x} = 0 \tag{3}$$

at the upstream limit of the hyperbolic zone.

The differential equation will admit discontinuous solutions of the form

$$\phi_x^+ + \phi_x^- = 0 \tag{4}$$

for a discontinuity normal to the x axis. Since the TSFOIL algorithm forces ϕ_{xx} to be zero at the sonic line it follows that

$$\phi_x^+ = \phi_x^- \tag{5}$$

Thus the only compatible solution is

$$\phi_x^+ = \phi_x^- = 0 \tag{6}$$

and the flow in at least the initial part of the hyperbolic domain is subsonic ($\phi_x < 1$). If the flow accelerates over the succeeding portion of the airfoil, as is usual, then it is possible that at the downstream limit of the hyperbolic domain the velocity is still subsonic, in which case an expansion shock wave must exist there. This is the situation in the computations shown in Figure 1. The anomaly is due to the enforcement of a continuous ϕ_x at the "sonic" line, a condition which is not a solution of the differential equation.

3.) Studies of the TSD Equation

3.1 Introduction

The TSD equation contains several of the features of the Euler equations, in particular the presence of shock waves. The equation is relatively easy to analyze compared to the Euler equations and will be used to provide insight into some of the problems arising in the linearization.

The mechanics of correctly linearizing the TSD equation are examined in detail in Reference 3. Basically the nonlinear TSD equation is expanded in a power series in a small parameter, ϵ, in terms of a coordinate system that is also perturbed as a series. This strained coordinate technique allows a valid perturbation even when shock waves move during the perturbation. The original work was for steady flow; a later extension is to unsteady flow (Ref. 4). The objective of this work was to perturb the airfoil geometry or the flow parameters to obtain a

solution in the neighborhood of the original base solution. The objective in the present work is to allow large perturbations from the base solutions and thus estimate the accuracy of the linearized TSD equation. The base solution need not be related to the problem under consideration other than by the fact that it has a supersonic zone with a shock wave. It is pointed out in Reference 3 that if the base solution does not have a shock wave then the linearized equation cannot have a shock wave.

The work reported in References 3 and 4 uses an integral equation analysis which allows a coupling of the boundary conditions and the velocities to form two coupled integral equations. These equations are easier to analyze than the basic partial differential equations and their associated boundary conditions. However, since the object of the present study is to extend the linearization techniques to the Euler equations, it is desirable to use finite difference methods because of their advanced state of development. Accordingly the study described in this section starts with a more detailed examination of the integral equation than that given in Reference 3 and then extends the basic ideas to finite difference methods.

The first result to emerge from the study is that the perturbation theory given in References 3 and 4 is in error, although the results are correct. The reasons are given later in this section. It is found that the shock location is such that oscillations in the neighborhood of the sonic line vanish. This criteria, found using the integral equation, applies to the finite difference formulation. As a consequence it is essential that the finite difference approximation does not, in general, remove these oscillations since their presence is critical to a correct location of the shock wave. In this section, results found using mixed differencing are incorrect because the difference scheme removes these oscillations, thus allowing the shock wave to be located anywhere.

Both the integral equation and the finite difference approximations are used to compute solutions of the linearized TSD equation, and these results are of adequate accuracy.

3.2 Basic Equations

The basic transonic small disturbance equation is

$$\phi_{xx} + \phi_{yy} = \phi_x \phi_{xx} \tag{7}$$

with the tangency boundary condition (for a symmetric airfoil)

$$\phi_y (x, \pm 0) = y_s'(x) \tag{8}$$

The far field boundary condition is that $\phi_{x'}$, $\phi_y \to 0$ at an infinite distance from the airfoil. Change the coordinates to (x',y') where

$$\begin{aligned} x' &= x + f(x,y) \\ y' &= y + g(x,y) \end{aligned} \tag{9}$$

The differential equation, Equation (7), can then be written as

$$\begin{aligned} \phi_{x'x'} + \phi_{y'y'} = {} & \phi_{x'}\phi_{x'x'} + \frac{1}{2}\frac{\partial}{\partial x'}\{[(1+f_x)\phi_{x'} + g_x\phi_{y'}]^2 - \phi_{x'}^2\} \\ & + f_x \frac{\partial}{\partial x'}\{[(1+f_x)\phi_{x'} + g_x\phi_{y'}]^2/2 - [(1+f_x)\phi_{x'} + g_x\phi_{y'}]\} \\ & + g_x \frac{\partial}{\partial y'}\{[(1+f_x)\phi_{x'} + g_x\phi_{y'}]^2/2 - [(1+f_x)\phi_{x'} + g_x\phi_{y'}]\} \\ & - f_y \frac{\partial}{\partial x'}[(1+g_y)\phi_{y'} + f_y\phi_{y'}] - g_y \frac{\partial}{\partial y'}[(1+g_y)\phi_{y'} + f_y\phi_x] \\ & - \frac{\partial}{\partial x'}[f_x\phi_{x'} + g_x\phi_{y'}] - \frac{\partial}{\partial y'}[g_y\phi_{y'} + f_y\phi_x] \end{aligned} \tag{10}$$

and the boundary condition becomes

$$\phi_y\ (x, \pm 0) = (1 + g_y)\ \phi_{y'} + f_y\ \phi_{x'} = y'_s\ (x(x')) \qquad (11)$$

Denote

$$(1 + f_x)\phi_{x'} + g_x\phi_{y'} \text{ by } U$$

$$(1 + g_y)\phi_{y'} + f_y\phi_{x'} \text{ by } V$$

Equations (10) and (11) can then be written in integral form using Green's identity to give

$$U - \frac{U^2}{2} = \frac{1}{2\pi} \int_0^1 \frac{\Delta[y'_s(\xi(\xi')) - f_\eta\phi_{\xi'}](x' - \xi')}{(x' - \xi')^2 + y'^2} d\xi'$$

$$- \int_S\int K_{\xi' x'} \left[\frac{U^2}{2} - f_\xi\ \phi_{\xi'} - g_\xi\phi_{n'}\right] dS$$

$$+ \int_S\int K_{x'} \left\{f_\xi \frac{\partial}{\partial\xi'} \left[\frac{U^2}{2} - U\right] + g_\xi \frac{\partial}{\partial\eta'} \left[U/2^2 - U\right] - \frac{\partial}{\partial\eta'} \left[g_\eta\phi_{\eta'} + f_\eta\phi_{\xi'}\right]\right.$$

$$\left. - f_\eta \frac{\partial}{\partial\xi'} V - g_\eta \frac{\partial}{\partial\eta'} V\right\} dS \qquad (12)$$

where

$$K\ (x,\xi;\ y,\eta) = \frac{1}{2\pi} \ln \{(x - \xi)^2 + (y - \eta)^2\} \qquad (13)$$

and S is the flow domain shown in Figure 2. Now let

$$\begin{aligned} U &= U_o + U_1 \\ V &= V_o + V_1 \end{aligned} \qquad (14)$$

where U_o and V_o are some specified velocities: Equation (12) then becomes

$$U_1(1 - U_o) - \frac{U_1^2}{2} = I_L - \int_S\int K_{\xi',x'}\{U_oU_1 + \frac{U_1^2}{2} - A\}dS$$
$$+ \int_S\int K_{x'}[f_\xi \frac{\partial}{\partial\xi'} + g_\xi \frac{\partial}{\partial\eta'}][(U_o + U_1) - (U_o + U_1)^2/_2]\}dS$$
$$- \int_S\int K_{x'}\{f_\eta \frac{\partial}{\partial\xi'}(V_o + V_1) + g_\eta \frac{\partial}{\partial\eta'}(V_o + V_1)\}dS$$
$$- \int_S\int K_{x'}\{\frac{\partial}{\partial\eta'} C\}dS \qquad (15)$$

where

$$I_L = \frac{1}{2\pi}\int_0^1 \frac{\Delta[y_s'(\xi(\xi')) - f_\eta B](x - \xi')}{(x' - \xi')^2 + y'^2}d\xi'$$
$$+ \frac{U_o^2}{2} - U_o - \int_S\int K_{\xi',x'}U_o^2/2\, dS \qquad (16)$$

and

$$\left.\begin{aligned} A &= \frac{(U_o + U_1)[f_\xi + f_\xi g_\eta - g_\xi f_\eta] + g_\xi(V_o + V_1)}{\{(1 + g_\eta)(1 + f_\xi) - f_\eta g_\xi\}} \\ B &= [(1 + g_\eta)(U_o + U_1) - g_\xi(V_o + V_1)]/[(1 + f_\xi)(1 + g_\eta) - f_\eta g_\xi] \\ C &= [(1 + f_\xi)(V_o + V_1) - f_\eta(U_o + U_1)]/[(1 + f_\xi)(1 + g_\eta) - f_\eta g_\xi] \end{aligned}\right\} \qquad (17)$$

The equations given above are exact; no approximations have been made. The velocities U_o, V_o are arbitrary. As a first approximation let

$$|U_1| << |U_o|$$
$$|V_1| << |V_o| \qquad (18)$$

such that the nonlinear terms in U_1 or V_1 can be neglected. Also, assume that products of U_1 and V_1 with derivatives of f and g can be neglected. This leads to the approximate form of the equation

$$U_1(1 - U_o) = I_L - \int_S \int K_{\xi',x'} \{U_o U_1 - \hat{A}\} dS$$

$$+ \int_S \int K_{x'} \{[f_\xi \frac{\partial}{\partial \xi'} + g_\xi \frac{\partial}{\partial \eta'}] [U_o - U_o^2/2] - \frac{\partial \hat{C}}{\partial \eta'}$$

$$- f_\eta \frac{\partial V_o}{\partial \xi'} - g_\eta \frac{\partial V_o}{\partial \eta'}\} dS \qquad (19)$$

and

$$\hat{A} = \frac{U_o[f_\xi + f_\xi g_\eta - g_\xi f_\eta] + g_\xi V_o}{[(1 + g_\eta)(1 + f_\xi) - f_\eta g_\xi]}$$

$$\hat{C} = [V_o (g_\eta + f_\xi g_\eta - f_\eta g_\xi) + f_\eta U_o]/[(1 + g_\eta)(1 + f_\xi) - f_\eta f_\xi] \qquad (20)$$

In the general cases discussed later the y straining is not a function of x and hence

$$g_\xi = 0 \qquad (21)$$

This leads to the simplified equation

$$U_1(1 - U_o) = \tilde{I}_L - \int_S \int K_{\xi',x'} \{U_o U_1 - \tilde{A}\} dS$$

$$+ \int_S \int K_{x'} \{f_\xi \frac{\partial}{\partial \xi'} [U_o - U_o^2/2]$$

$$- \frac{\partial \tilde{C}}{\partial \eta'} - f_\eta \frac{\partial V_o}{\partial \xi'} - g_\eta \frac{\partial V_o}{\partial \eta'}\} dS \qquad (22)$$

and

$$\left.\begin{aligned} \tilde{A} &= \frac{U_o f_\xi (1 + g_\eta)}{[(1 + g_\eta)(1 + f_\xi)]} \\ \tilde{C} &= \frac{[V_o g_\eta (1 + f_\xi) + f_\eta U_o]}{[1 + g_\eta)(1 + f_\xi)]} \end{aligned}\right\} \qquad (23)$$

$\tilde{I}_L$ is the same as I_L defined in Equation (16) but with B replaced by $\tilde{B}$.

where

$$\tilde{B} = U_o / (1 + f_\xi) \qquad (24)$$

The next step in simplification is that the coordinate straining terms f, g are small and expressions containing them can be linearized. Thus, Equation (22) reduces to

$$\begin{aligned} U_1(1 - U_o) = \bar{I}_L &- \int_S \int K_{\xi', x'} \{U_o U_1 - f_\xi U_o\} dS \\ &+ \int_S \int K_{x'} \{f_\xi, \frac{\partial}{\partial \xi'} (U_o - U_o^2/2) - \frac{\partial}{\partial \eta'} (g_\eta V_o) - \frac{\partial}{\partial \eta'} (f_\eta U_o) \\ &f_\eta \frac{\partial V_o}{\partial \xi'} - g_\eta \frac{\partial V_o}{\partial \eta'}\} dS \end{aligned} \qquad (25)$$

and

$$\bar{I}_L = \frac{1}{2\pi} \int_0^1 \frac{\Delta[y_s'(\xi') + f\, y_s'(\xi')](x' - \xi')}{[(x' - \xi')^2 + y'^2]} d\xi' \qquad (26)$$

Equation (25) is further simplified by neglecting f_η and putting g zero. The first of these assumptions implies that the straining does not vary significantly with y; the second indicates there is no straining in the y direction.

Neglecting f_η and g, Equation (25) can be written as

$$U_1(1 - U_o) = I_{L1} - \int_S \int K_{\xi',x} U_o U_1 dS + \delta x_s I_f \tag{27}$$

where

$$I_{L1} = \frac{1}{2\pi} \int_o^1 \frac{\Delta y_s' (\xi')(x' - \xi')}{[(x' - \xi')^2 + y'^2]} d\xi \tag{28}$$

$$I_f = \int_S \int K_{\xi',x'} \bar{f}_{\xi'} U_o \, dS + \int_S \int K_{x'} \bar{f}_{\xi'} \frac{\partial}{\partial x'} (U_o - U_o^2/2) dS$$

$$+ \frac{1}{2\pi} \int_o^1 \frac{\Delta \bar{f} \, y_s'' (\xi')(x' - \xi')}{(x-\xi')^2 + y'^2} d\xi \tag{29}$$

and

$$\bar{f} = f/\delta x_s \tag{30}$$

where δx_s is some parameter related to the shock location.

3.3 Analysis

Equation (27) can be written in the form

$$U_1 (1 - U_o) = I_{L1} + I_{s1} + \delta x_s I_f \tag{31}$$

where I_s is the double integral in Equation (27). This is an equation for the unknowns U_1 and δx_s. If the integrals in Equation (31) are discretized then, if there are N_x points in the x direction and N_y points in the y direction, Equation (31) becomes a set of N_T algebraic equations for N_T values of U_1 and N_s values of δx_s where

$$N_T = N_x N_y \tag{32}$$

and N_s is the number of y grid lines covering the supersonic zone in U_o. It can be seen therefore that if there is a supersonic zone in U_o then there is an insufficient number of equations to solve for the $N_T + N_S$ unknowns. The additional equations are obtained by differentiating Equation (31) with respect to x to give

$$U_{1x}\,(1 - U_o) - U_{ox}U_1 = \frac{\partial}{\partial x}\{I_{L1} + I_{s1}\} + \delta x_s \frac{\partial I_f}{\partial x} \tag{33}$$

If U_{1x} is finite when $U_o = 1$, that is U_1 does not constitute an expansion shock, then at x^* (the value of x when $U_o = 1$) Equation (33) gives

$$- U^*_{ox}\, U^*_1 = \frac{\partial}{\partial x}\{I_{L1} + I_{s1}\}|_{x=x^*} + \delta x_s \{\frac{\delta I_f}{\partial x}\}|_{x=x^*} \tag{34}$$

If the integrals are discretized as before then Equation (34) gives N_s equations for the N_s values of δx_s in terms of U_1. Hence, Equations (31) and (34) are sufficient to solve for U_1 and δx_s.

The above description of the shock locating mechanism is adequate for the integral equation formulation but does not really provide much insight into how the shock is located in a finite difference formulation of the TSD equation. Accordingly some further investigation into the nature of the mechanism of the shock location is necessary.

Equation (31) is an equation for U_1 and, if the integrals are discretized, then the following matrix equation results

$$A_{ij}\, U_{1j} = B_i + \delta x_s\, C_i \tag{35}$$

where B_i is a matrix of I_{L1} and C_i the matrix of I_f at the "i"th. grid point and U_{ij} is the value of U_1 at the jth grid point.

Equation (35) can be inverted to give

$$U_{1j} = A_{ij}^{-1} B_i + A_{ij}^{-1}[\delta x_s C_i] \tag{36}$$

and some criterion must be used to select δx_s.

In the integral formulation, Equation (34) can be used in conjunction with Equation (31) to give a modified equation

$$\tilde{A}_{ij} U_{1j} = \tilde{B}_i \tag{37}$$

where $\tilde{A}_{ij}U_{1j}$ is a representation of the term

$$U_1(1 - U_o) + \int_S \int K_{\xi',x'} U_o U_1 \, dS - \{U_1^* U_{o_x}^* - [\int_S \int K_{\xi',x',x'} U_o U_1 dS]^*\} I_f / I_{f_{x'}}^*$$

and B_i is a representation of the term

$$B_i - I_{L1_{x'}}^* I_f / I_{f_{x'}}^*$$

It would appear that the use of Equation (36) would give some insight into the nature of the shock fitting. Consequently the matrix A_{ij} was assembled and each of the terms on the right hand side computed.

In order to allow for a variable shock movement the matrix C_i is split into components $C_i^{(k)}$ where

$$C_i = \sum_{k=1}^{N_s} C_i^{(k)} \tag{38}$$

and N_s is the number of grid points in the supersonic domain. The matrix $C_i^{(k)}$ contains only those values of C_i on the kth grid line with the rest of its elements zero. When k is equal to N_s the matrix $C_i^{(N_s)}$ contains all of the elements in the outer subsonic domain in addition to those on the N_sth y grid line. Thus Equation (36) can be written as

$$U_{lj} = A_{ij}^{-1} B_i + \sum_{k=1}^{N} \delta x_{s_k} A_{ij}^{-1} C_i^{(k)} \tag{39}$$

In Figure 3 the term $A_{ij}^{-1} B_i$ is shown and exhibits oscillations. This is equivalent to a solution without moving the shock wave.

If Equation (37) is solved, the result for U_{lj} is smooth, as shown in Figure 4. If the values of δx_{s_k} calculated during this solution are used in conjunction with Equation (39) then the term

$$\sum_{k=1}^{N} \delta x_{s_k} A_{ij}^{-1} C_i^{(k)}$$

oscillates as is shown in Figure 5. However, the sum of both the terms on the right hand side of Equation (39) leads to the U_{lj} shown in Figure 4.

From the preceding discussion it follows that the correct shock location is the location that removes the oscillations. An alternative way of locating the shock wave is to remove the oscillation in the solution of Equation (39). One method of achieving this is to enforce the condition

$$\left.\frac{\partial^3 U}{\partial x^3}\right|_{x^*} = 0 \tag{40}$$

on each y grid line that has a sonic point, x^*. This condition forces the solution U in the neighborhood of x_* to have curvature of constant sign, thus disallowing the oscillatory behavior. The example shown in Figure 4 was recalculated using Equation (40) rather than Equation (34) to locate the shock wave. The results of both methods were almost identical.

Some test cases were computed using Equations (31) and (34) as a basis. In all the cases the base solution is a 10% biconvex airfoil at $M_\infty = 0.808$. A single straining function of the type given in Reference 3 is used. In Figure 6 the pressure distribution around a NACA 0010 airfoil at $M_\infty = 0.808$ is shown, and it may be seen that the agreement with the direct solution is fair. However, considering the magnitude of the perturbation from the base solution, the agreement with the direct result is more startling. A similar remark can be made about the result shown in Figure 7 where the pressure distribution around a NACA 64A006 airfoil at $M_\infty = 0.875$ is shown.

In the original papers on the strained coordinate method, Equation (34) and its unsteady flow equivalent is not used. However, the solution around the sonic point was obtained by a second order interpolation using neighboring points. This interpolation actually enforces Equation (40) and hence the results of References 3 and 4 are correct, although the theory given in their papers is incomplete since it does not explicitly discuss the use of a condition like that of Equation (34) or Equation (40). In the following discussion the causes of these oscillations are examined.

3.4 Origin of the Oscillatory Behavior

If there is no shock term, that is δx_s is zero, then Equation (31) can be discretized on a uniform grid to give

$$U_i \ (1 - U_{oi}) = \sum_{j=1}^{N_T} f_{ij} \ U_{ij} \ \Delta\xi + B_i \qquad (41)$$

where B_i is the value of I_{Li} at the grid point i and $f_{ij}\,\Delta\xi$ is an influence function that gives the contribution of U_j at the jth point to the ith point.

Velocity perturbations at points i and i + 1 on a uniformly partitioned grid are given as

$$U_i[(1 - U_{oi}) - f_{i,i}\Delta\xi] = \sum_{\substack{j=1 \\ j\neq i,i+1}}^{N_T} f_{i,j}U_j\,\Delta\xi + f_{i,i+1}U_{i+1}\Delta\xi + B_i \tag{42}$$

$$U_{i+1}[(1- U_{o_{i+1}}) - f_{i+1,i+1}\Delta\xi] = \sum_{\substack{j=1 \\ j\neq i,i+1}}^{N} f_{i,j}\,U_j\,\Delta\xi + f_{i+1,i}\,U_i\Delta\xi + B_{i+1} \tag{43}$$

If $\Delta U = U_{i+1} - U_i$, then ΔU can be expressed as

$$\Delta U = \frac{A[\Delta\xi(f_{i+1,i}- f_{i,i+1})-(C_{i+1}- C_i)]-\Delta\xi(B_{i+1}f_{i,i+1}-B_i f_{i+1,i})+C_i B_i}{(C_i C_{i+1}-f_{i,i+1}f_{i+1,i}(\Delta\xi)^2)}$$

where (44)

$$C_i = (1 - U_{o_i}) - f_{i,i}\,\Delta\xi \text{ and } A = \sum_{\substack{j=1 \\ j\neq i,i+1}}^{N} f_{i,j}\,U_j\,\Delta\xi.$$

Expanding all variables at the point i+1 in terms of their value at the point i, using a Taylor series expansion, and neglecting the terms with second or higher order of $\Delta\xi$ the following relation is obtained;

$$\Delta U = \frac{(A+B_i)\left.\frac{\Delta U_o}{\Delta\xi}\right|_i \Delta\xi + (1-U_{o_i})\left.\frac{\Delta B}{\Delta\xi}\right|_i \Delta\xi}{(1-U_{o_i})^2 - (1-U_{o_i})\left.\frac{\Delta U_o}{\Delta\xi}\right|_i \Delta\xi} \tag{45}$$

Next consider Equation (42) and note that

$$U_i(1-U_{o_i}) = A + [f_{i,i}\, U_i + f_{i,i+1}(U_i + \frac{\Delta U}{\Delta \xi}\Big|_i \Delta\xi)]\, \Delta\xi + B_i \qquad (46)$$

To the lowest order, consistent with the order of Equation (45), Equation (46) can be reduced to

$$A + B_i = U_i(1 - U_{oi}) - (f_{i,i} + f_{i,i+1})\, U_i\, \Delta\xi. \qquad (47)$$

Substituting this relation in Equation (45) and neglecting terms of $(\Delta\xi)^2$ the following equation is obtained.

$$\Delta U^+ = U_{i+1} - U_i = \frac{U_i \frac{\Delta U_o}{\Delta \xi}\Big|_i \Delta\xi + \frac{\Delta B}{\Delta \xi}\Big|_i \Delta\xi}{(1-U_{o_i}) - \frac{\Delta U_o}{\Delta \xi}\Big|_i \Delta\xi} \qquad (48)$$

A similar procedure can be used to show that

$$\Delta U^- = U_i - U_{i-1} = \frac{U_i \frac{\Delta U_o}{\Delta \xi}\Big|_i \Delta\xi + \frac{\Delta B}{\Delta \xi}\Big|_i \Delta\xi}{(1-U_{o_i}) + \frac{\Delta U_o}{\Delta \xi}\Big|_i \Delta\xi} \qquad (49)$$

and it can be seen that $\Delta U^+ \neq -\Delta U^-$. If $U_{o_i} \neq 1$ then ΔU^+ and ΔU^- approach zero as $\Delta\xi \to 0$ and hence $|\frac{\partial U}{\partial \xi}|$ is finite.

If

$$U_{o_i} = 1, \qquad (50)$$

that is, at the sonic point,

then

$$\Delta U^{+} = -\Delta U^{-} = U_i + \left(\frac{\Delta B}{\Delta \xi}\Big|_i\right)/\left(\frac{\Delta U_o}{\Delta \xi}\Big|_i\right) \tag{51}$$

Hence U oscillates about the sonic point since

$$U_{i-1} - U_i = U_{i+1} - U_i$$

Furthermore, as $\Delta\xi \to o$, $\Delta U \neq o$ and hence

$$\left(\frac{\partial U}{\partial \xi}\right)_{\text{sonic}} \to \infty \tag{52}$$

which is an expansion shock.

A measure of the amplitude of the oscillation is given by the second derivative, which gives in discretized form

$$\Delta U^{+} - \Delta U^{-} = \frac{2\left(\frac{\Delta U_o}{\Delta \xi}\Big|_i\right)\left[U_i \frac{\Delta U_o}{\Delta \xi}\Big|_i + \frac{\Delta B}{\Delta \xi_i}\Big|_i\right]\Delta \xi^2}{(1-U_{o_i})^2 - \left(\frac{\Delta U_o}{\Delta \xi}\Big|_i\right)^2 \Delta \xi^2} \tag{53}$$

If $\frac{\Delta U_o}{\Delta \xi}\Big|_i$ and $\frac{\Delta B}{\Delta \xi}\Big|_i$ are considered constant then the amplitude decays as $\frac{1}{(1-U_{o_i})^2}$ increases. In other words, the oscillations decrease the further the point ξ_i is from the sonic point.

The conclusions reached by this analysis are consistent with the computational evidence shown earlier.

3.5 Multiple Coordinate Straining

It had been intended to use a multiple straining of the coordinates so that both the shock and the sonic line location could be changed; the sonic line location can be fixed at the location of the sonic line in the base solution U_o. This multiple straining would ensure that the hyperbolic domain in both the perturbed and base solutions would be identical in the strained coordinate system. Preliminary tests of this idea did not prove fruitful, and a modified version of the idea was investigated. Briefly, this modification consisted of evaluating the second straining parameter to minimize a weighted sum of the $|U_{1i}|$ over the solution. The rationale is that since the $|U_{1i}|$ is a minimum in some average sense, then the error in the linearization process, which is of the order of $|U_{1i}^2|$, would be a minimum, thus improving the overall accuracy of the solution. A preliminary example is shown in Figure 8 where the pressure distribution over a NACA0010 airfoil at a Mach number of 0.808 is shown. It can be seen that the effect of the second straining is considerable. However, this is a preliminary result and further work is necessary to consolidate the concept of using an extra straining to improve the accuracy of the solution.

3.6 Summary

In this section the concept of using the linearized TSD equation to model transonic flow is examined. The method does appear feasible. The shock wave is located by requiring that no expansion shocks can occur in the solution, and two methods of enforcing this condition with the integral equation method are derived. One form of this condition, Equation (40), can be used in conjunction with a finite difference solution of the TSD equation in differential form.

3.7 Linearized Solutions of the Differential TSD Equation

In its simplest form the linearized TSD equation, equivalent to Equation (27), can be written as

$$(1-U_o)\,\phi_{1x'x'} - U_{o_{x'}}\phi_{1x'} + \phi_{1yy} = \frac{1}{2}\frac{\partial}{\partial x'}\{[(1+f_x)\phi_{ox'}]^2 - \phi_{ox'}^2\} + f_x\frac{\partial}{\partial x'}\{\frac{\phi_{ox'}^2}{2} - \phi_{ox'}\} \tag{54}$$

with the tangency boundary condition

$$\left.\begin{aligned}\phi_{1y}(x', \pm 0) &= y_s'(x(x')) - y_{so}'(x') \\ &= y_s'(x') - y_{so}'(x') - f\,y_s'(x')\end{aligned}\right\} \tag{55}$$

To investigate the solution of this equation the computer code TSFOIL (Ref. 5) is used. TSFOIL uses mixed upwind and central differencing to solve the nonlinear TSD equation, Equation (1), and special parabolic and shock point operators to allow a conservative transfer from one scheme to the other. The parabolic point operator essentially eliminates expansion shocks by insuring that

$$\phi_{yy} = 0 \tag{56}$$

when $\phi_x = 1$. This condition forces ϕ_{xx} to be finite. If this mixed difference scheme is applied to the left hand side of Equation (54), that is, the straining term is zero, and the term $U_{ox'}\,\phi_{1x'}$ is evaluated with central differences then the shock jump condition is

$$U_1^+ + U_1^- = \Delta x U_{1x}^+ \tag{57}$$

compared to the theoretical condition

$$U_1^+ + U_1^- = 0 \tag{58}$$

The shock jump $[U_1]$ is given by

$$[U_1] = 2U_1^+ - \Delta x U_{1x}^+ \tag{59}$$

Equation (54) with f put equal to zero was solved using the mixed difference scheme described above and the pressure distribution around an 11% biconvex airfoil at $M_\infty = 0.808$ is shown in Figure 9. The base solution is a 10% biconvex airfoil at the same Mach number. It can be seen that the linearized result is smooth and that the shock is located at the wrong position since it is still at the base position. There are no oscillations in the pressure distributions in the neighborhood of the sonic line and consequently no apparent mechanism to correctly locate the shock wave. In this case the difference scheme, which smooths oscillatory behavior, has eliminated the oscillations which indicate an incorrect shock location. The mixed difference scheme can give plausible but incorrect solutions. The weakened shock jump is explained by the modified jump condition given by Equation (59).

In order to obtain the correct behavior, Equation (54) is solved using central differencing everywhere. The result, without straining, is shown in Figure 10 and it may be seen that the solution oscillates in the neighborhood of the sonic point. If the straining terms are included and evaluated using Equation (40) then the solution is smooth in the region of the sonic lines can be seen in Figure 11.

A second example, using central differencing, is shown in Figures 12 and 13 where the pressure distribution over a NACA0010 airfoil is shown. Figure 12 shows the result without coordinate straining and Figure 13 the result with coordinate straining. The Mach number and base solution are the same as for the previous example.

The grid used in these computations is relatively coarse in the y direction (14 points) because of computer storage problems. This may account for the variable accuracy of the calculations.

From the discussions above it can be inferred that the finite difference algorithm used to solve the TSD equation must be nondissipative so as to allow oscillations to occur in the neighborhood of the sonic line. These oscillations are removed by locating the shock wave in the correct position. The fact that the dissipative algorithm gives a plausible but incorrect solution should be a warning. It is imperative that the mathematical aspects of the differential equation being solved are understood before a choice of algorithm is made.

4.) Linear Perturbation Equations with Constant Coefficients

4.1 Introduction

One of the problems that arise in the previously reported method for linearizing the transonic small disturbance (TSD) equation is that the number of shock waves in the solution is fixed by the base solution. Since transonic flows can have multiple shocks, this is a severe restriction on the method since the number of shocks in a solution must be known a priori. A second problem is the behavior at the sonic line which is different in a finite difference approximation of the TSD equation than in the mathematical formulation. In the former oscillations appear in the neighborhood of the sonic line, while in the mathematical picture an expansion shock forms. If the solution could be linearized about two constant velocities, one supersonic and one subsonic, then these problems would be reduced. Since the transonic solution would now consist of combining any number of elements of the supersonic solution into a subsonic solution, the shock being represented by a jump from the supersonic solution to the subsonic solution, any number of shocks could be incorporated into the solution. Also, since the

base solutions do not pass continuously through sonic conditions the problem at the sonic line would disappear. The following analysis suggests a method of implementing this idea.

4.2 Basic Equations

The integral equation for the velocity, u, can be written in an arbitrary coordinate system as

$$u - \frac{u^2}{2} = I_L + I(u^2/2) + \delta x_o\, I_g + \delta x_s\, I_f + \delta y_s I_h \qquad (60)$$

where I_L is the Prandtl-Glauert velocity, I is a field integral and I_g, I_h and I_f are functions from a three point coordinate straining with δx_o, δx_s being straining in the x-axis and δy_s a straining in the y-axis. The terms $I(u^2/2)$, I_g, I_f, I_h are continuous and possess continuous first derivatives. Sonic conditions occur when u is unity.

Now let

$$u = u_o + u_1 \qquad (61)$$

where u_o is either 0 (a subsonic value) or 2 (a supersonic value).

Equation (60) can now be written as

$$(u_o + u_1)\,(1 - u_o) = I_L + I\,(\frac{u_1^2}{2}) + I[(u_o + u_1)\,u_o] - I(u_o^2/2)$$

$$+ \frac{u_1^2}{2} - \frac{u_o^2}{2} + \delta x_s\, I_f + \delta x_o\, I_g + \delta y_s\, I_h \qquad (62)$$

Let an * denote values on a sonic line, $(u_o + u_1 = 1)$.

Equation (62) can be written as

$$(u_o + u_1)\,(1 - u_o) = F + \frac{u_1^2}{2} - u_o^2/2 \qquad (63)$$

where F is a continuous function. The main object is to determine where the solution should transfer from the subsonic solution to the supersonic solution and vice versa.

Let u_o jump from zero to two at some x^* and from two to zero at x_s.

Differentiation of Equation (63) gives

$$(u_o + u_1)_x\,(1 - u_o) - u_{ox}(u_o + u_1) = F_x + u_1 u_{1x} - u_o u_{ox} \qquad (64)$$

or

$$(u_o + u_1)_x\,(1 - u_o - u_1) = F_x \qquad (65)$$

If the condition that $u_o + u_1$ passes smoothly though unity is imposed, Equation (66) gives the shock condition of the classic integral equation.

Now linearize Equation (63) about u_o; thus

$$(u_o + u_1)\,(1 - u_o) = \bar{F} - u_o^2/2 \qquad (66)$$

where $\bar{F}$ is a linearized version of F.

It is desired that on either side of x^*, $u_o + u_1$ is unity (sonic). Thus,

$$(u_o + u_1)^- = \bar{F}^* = -\,(\bar{F}^* - 2) = (u_o + u_1)^+ = 1 \qquad (67)$$

or

$$\bar{F}^{*} = 1 \tag{68}$$

where the "+" and "-" superscripts denote values just ahead of and behind x^{*} respectively, Equation (68) will give an equation for the shock location

Differentiation of Equation (66) gives

$$(u_o + u_1)_x (1 - \tilde{u}_o) - \tilde{u}_1 u_{o_x} = \bar{F}_x \tag{69}$$

where a tilde denotes an average value at the point of differentiation. Since u_{ox} is infinite at x^{*} (it is a delta function) and since $(u_o + u_1)_x$ is required to be bounded and $\bar{F}_x$ is finite it follows that

$$\tilde{u}_1^{*} = 0 \tag{70}$$

If $u_{o_x} + u_{1_x}$ is to be finite at x^{*}, then since u_{ox}^{*} is infinite

$$u_{1_x}^{*} = - u_{o_x}^{*} \tag{71}$$

Since u_{ox}^{*} is the derivative of a step of magnitude 2 it follows that u_{1x}^{*} is the derivative of a step of magnitude 2. Using this information and Equation (70) it follows that

$$u_1^{-} = 1, \; u_1^{+} = -1, \; \tilde{u}_1^{*} = 0 \tag{72}$$

hence, the condition that $u_{ox} + u_{1x}$ be finite leads to the result that the sonic line occurs at x^{*}. In other words the linearization of the equation makes the sonic line at x^{*}. Since x^{*} can be put anywhere it follows that the sonic line location is

arbitrary. It is only accurate if the (neglected) nonlinear terms in Equation (64) cancel. That is if

$$-\tilde{u}_1^* \tilde{u}_{1_x}^* = I^*_x(u_1^2/2) \tag{73}$$

From Equations (62) and (63)

$$\begin{aligned} u_1(1 - u_o) &= I_L + I(u_1 u_o) + [I(u_o^2/2) - u_o + u_o^2/2] \\ &\quad + \delta x_s\, I_f + \delta x_o\, I_g + \delta y_s\, I_h \\ &= \hat{F} \end{aligned} \tag{74}$$

where $\hat{F}$ is continuous. Expanding Equation (74) as a Taylor series about x^* gives

$$\begin{aligned} u_1^+ &= \hat{F} - \Delta x \hat{F}_x \\ u_1^- &= -(\hat{F} + \Delta x\, \hat{F}_x) \end{aligned} \tag{75}$$

Thus

$$\tilde{u}_1^* \tilde{u}_{1_x}^* = \frac{(-2\Delta x \hat{F}_x^*)}{2} \quad \frac{(-2\ \hat{F}^*)}{2\Delta x} = \hat{F}_x^*\ \hat{F}^* = \hat{F}_x^* \tag{76}$$

where it has been noted that $\hat{F}^* = 1$.

It can be seen that $\tilde{u}^*_1\ \tilde{u}^*_{1x}$ is actually a first order quantity. Hence, a linearized version of Equation (73) is

$$\hat{F}_x^* = 0 \tag{77}$$

Consider now Equation (66) at values just ahead of and behind the "sonic" line and denoted by the superscripts "+" and "-" respectively. On addition,

$$\frac{1}{2}\left[(u_o + u_1)^+ + (u_o + u_1)^-\right] = \frac{1}{2}\left[\bar{F}^+ + \bar{F}^-\right] - 1 \qquad (78)$$

or, since $\bar{F}$ is continuous,

$$\bar{F}^* = 0 \qquad (79)$$

Finally, let the shock and the sonic line coincide at the point (x_s, y_s) (the "top" of the "shock" in u_o). This gives

$$(\delta x_o + x_o)|_{y_s} = (\delta x_s + x_s)|_{y_s} \qquad (80)$$

Thus the governing equations are Equation (66) with Equation (79) applied at x^*, Equation (69), Equation (77), and Equation (80). These are sufficient for solving u, at N discrete points, δx_o, δx_s on each grid line and δy_s.

As a first approximation the δy_s term is neglected and only Equations (66), (69), (77), and (79) need be solved.

4.3 Possibility of Deriving a Closed Form Solution

In the classic strained coordinate theory I_f, I_g, I_h are evaluated using the base velocity, u_o. However, since u_o is piecewise constant it is instructive to use the unknown $(u_o + u_1)$ in this evaluation.

Consider the equation

$$(1 - u_o)\,\phi_{xx} + \phi_{yy} = 0 \qquad (81)$$

Since u_o is constant, Equation (81) can be written as

$$\phi_{x'x'} + \phi_{yy} = (u_o\phi_{x'})_{x'} + [(u_o-1)f_x\phi_{x'}]_{x'} - f_x(1 - u_o)[(1+f_x)\phi_{x'}]_{x'}, \quad (82)$$

where

$$x' = x + f(x) \quad (83)$$

In the general coordinate straining, x′ is given by

$$x = x' + x_1(x') \quad (84)$$

and

$$\phi_x = (1 + f_x)\phi_{x'} \quad (85)$$

It follows from Equations (83) and (84) that

$$1 + f_x = \frac{1}{1+x_{1_{x'}}} \quad (86)$$

and hence Equation (82) becomes

$$\phi_{x'x'} + \phi_{yy} = (u_o\phi_{x'})_{x'} + [x_{1_{x'}}(1 - u_o)\phi_x]_{x'} \left(\frac{x_{1_{x'}}}{1+x_{1_{x'}}}\right)(1 - u_o)\phi_{xx}, \quad (87)$$

If the terms involving $x_{1_{x'}}$ are linearized, then Equation (87) becomes

$$\phi_{x'x'} + \phi_{yy} = (u_o\phi_{x'})_{x'} + [x_1x' (1 - u_o) \phi_x]_{x'}$$

$$+ x_{1_{x'}} (1 - u_o)\phi_{xx'} \qquad (88)$$

Equation (88) can be regarded as a piecewise application of the subsonic and supersonic Prandtl Glauert equations in a strained coordinate system. Thus in the subsonic domain, Dsub, the equation is

$$\phi_{x'x'} + \phi_{yy} = [x_{1x'} \tilde{\phi}_{x'}]_{x'} + x_{1x'} \tilde{\phi}_{x'x'} \qquad (89)$$

and in the supersonic domain, Dsup, the equation is

$$-\phi_{x'x'} + \phi_{yy} = - [x_{1x'} \tilde{\phi}_{x'}] - x_{1x'}\tilde{\phi}_{x'x'} \qquad (90)$$

where $\tilde{\phi}_{x'}$ is some suitable (zeroth order) approximation to $\phi_{x'}$. These equations could be solved piecewise analytically in specified subdomains, Dsub, Dsup, with the matching condition of Equation (72) together with the condition

$$v^+ = v^- \qquad (91)$$

This second condition is implicit in the derivation of the integral equation, Equation (62). Both of these conditions are sufficient to choose a strained coordinate system but, as in the case of the integral equations, the sonic line will always be at x^*. It is not clear how a condition similar to Equation (73) can be implemented the differential form of the equation, and because of this a purely analytic solution of Equations (89) and (90) is probably useless.

4.4 Results

Some results were found using the integral equation theory with a triangular hyperbolic region. The height of the region was kept fixed, that is , no y straining is used. The hyperbolic domain closely resembles that for the 10% biconvex airfoil at $M_\infty = 0.808$. The pressure distribution over a NACA0010 at $M_\infty = 0.808$ is calculated and shown in Figure 14. The straining terms are evaluated using the base solution. A second result is shown in Figure 15; in this case the straining terms are evaluated using an estimate of the final, smooth solution. The results are very sensitive to small changes in I_L, and it is not suggested that this is a viable computation procedure. However, considering the size of the perturbation from the base solution, the accuracy of the results is surprising.

5. Perturbation of the Euler Equations

5.1 Introduction

In section (3) a method of locating the shock wave in the linearized TSD equation that is suitable for finite difference solutions is derived. If these ideas are extended to solutions of the linearized Euler equations in this section, it is found that the shock wave can be located correctly but only if the odd and even points are separated in the solution.

5.2 Basic Equations

The Euler equations can be written in general coordinates (ξ, η) as

$$\frac{\partial \hat{E}}{\partial \xi} + \frac{\partial \hat{F}}{\partial \eta} = 0 \qquad (92)$$

where

$$\hat{E} = J^{-1} \begin{bmatrix} \rho U \\ \rho uU + \xi_x p \\ \rho vU + \xi_y p \\ (\rho e + p)U \end{bmatrix} ; \hat{F} = J^{-1} \begin{bmatrix} \rho V \\ \rho uV + \eta_x p \\ \rho vV + \eta_y p \\ (\rho e + p)V \end{bmatrix} \tag{93}$$

where (x, y) is a cartesian coordinate system with velocity components u, v in the x and y directions respectively, p is pressure, ρ is density and e is given by

$$e = e_I + \frac{1}{2} q^2 \tag{94}$$

where e_I is the internal energy and q is the total velocity. U and V are given by

$$\left.\begin{aligned} U &= \xi_x u + \xi_y v \\ V &= \eta_x u + \eta_y v \end{aligned}\right\} \tag{95}$$

ρ, u, v are normalized with respect to freestream values, denoted by the subscript ∞, and p and ρe are normalized by $\rho_\infty q_\infty^2$. J is the Jacobian defined by

$$J = \xi_x \eta_y - \xi_y \eta_x \tag{96}$$

Equation (92) can be written as

$$\frac{\partial}{\partial \xi} [\hat{A} (\hat{Q}) \hat{Q}] + \frac{\partial}{\partial \eta} [\hat{B} (\hat{Q}) \hat{Q}] = 0 \tag{97}$$

where

$$\hat{Q} = J^{-1} [\rho, \rho u, \rho v, e]^T \tag{98}$$

and

$$\hat{A} = \begin{bmatrix} 0 & \xi_x & \xi_y & 0 \\ -uU + \xi_x\phi^2 & U + (2 - \gamma)\xi_x u & \xi_y u - (\gamma - 1)\xi_x v & (\gamma - 1)\xi_x p \\ -vU + \xi_y\phi^2 & \xi_x v - (\gamma - 1)\xi_y u & U + (2 - \gamma)\xi_y v & (\gamma - 1)\xi_y p \\ U[\phi^2 \mp a_1] & \xi_x a_1 - (\gamma - 1)uU & \xi_y a_1 - (\gamma - 1)vU & \gamma U \end{bmatrix} \tag{100}$$

$$\hat{B} = \begin{bmatrix} 0 & \eta_x & \eta_y & 0 \\ -uV + \eta_x\phi^2 & V + (2 - \gamma)\eta_x u & \eta_y u - (\gamma - 1)\eta_x v & (\gamma - 1)\eta_x p \\ -vV + \eta_y\phi^2 & \eta_x v - (\gamma - 1)\eta_y u & V + (2 - \gamma)\eta_y v & (\gamma - 1)\eta_y p \\ V[\phi^2 \mp a_1] & \eta_x a_1 - (\ \ - 1)uV & \eta_y a_1 - (\gamma - 1)vV & \gamma V \end{bmatrix}$$

where

$$a_1 = \gamma e/\rho - \phi^2;\ \phi^2 = (\gamma - 1)\ (u^2 + v^2)/2 \tag{101}$$

and

$$\hat{A} = \frac{\partial \hat{E}}{\partial \hat{Q}},\ \hat{B} = \frac{\partial \hat{F}}{\partial \hat{Q}} \tag{102}$$

For a nonlifting airfoil, the numerical solution of Equation (97) requires the following boundary conditions.

On the far field boundary, freestream values are imposed on all variables; this is valid strictly only for isentropic flows. On the body surface, $\eta = 0$,

$$\left.\begin{aligned} v &= 0 \\ \frac{\partial \rho}{\partial \eta} &= 0 \\ \frac{\partial U}{\partial \eta} &= 0 \\ \frac{\partial e}{\partial \eta} &= 0 \end{aligned}\right\} \qquad (103)$$

These boundary conditions impose zero vorticity on the airfoil surface, again valid only for isentropic flow. Although the imposed boundary conditions leave something to be desired, it is expected that useful insight into the solution of the linearized Euler equations can be gained.

5.3 Linearized Euler Equations

The linearization of Euler equations used in the present analysis is designed to be similar to that used for the TSD equation and, in fact, reduces to the perturbed TSD equation if the correct limiting processes are used.

Equation (97) is written in a general coordinate system so if the x coordinate is strained such that

$$x = x' + \epsilon x_1(x') \qquad (104)$$

where (x',y) is the strained coordinate system with a straining parameter, δ_{xs}, then the effect can be felt only through the Jacobian, J.

The coordinates are strained as follows

$$\left.\begin{aligned} \xi(x, y) &= \xi(x', y) \\ \eta(x, y) &= \eta(x, y) \end{aligned}\right\} \qquad (105)$$

such that

$$\left.\begin{aligned} \xi_x &\sim \xi_{x'} - \epsilon x_{1x'}\, \xi_{x'} \\ \eta_x &\sim \eta_{x'} + \epsilon x_1 \eta_{x'x'} \end{aligned}\right\} \tag{106}$$

The relations of Equations (105) and (106) are similar to those used in the TSD theory. The general variable Q is expanded as

$$Q = Q_o + \epsilon Q_1 \tag{107}$$

where

$$Q = [\rho,\ \rho u,\ \rho v,\ e]^T \tag{108}$$

The Jacobians $\hat{A}$, $\hat{B}$ can be written as

$$\left.\begin{aligned} \hat{A} &= \hat{A}_o(Q_o) + \epsilon \hat{A}_1(Q_o) \\ \hat{B} &= \hat{B}_o(Q_o) + \epsilon \hat{B}_1(Q_o) \end{aligned}\right\} \tag{109}$$

where $\epsilon\hat{A}_1$ and $\epsilon\hat{B}_1$ are the perturbations of $\hat{A}$ and $\hat{B}$ respectively due to a change in ξ_x, η_x only.

Finally, the Jacobian J is expanded as

$$J = J_o + \epsilon J_1 \tag{110}$$

Substitution of Equations (107), (109), and (110) yield the following perturbation equations

$$\frac{\partial}{\partial \xi}\left[\hat{A}_o(\hat{Q}_o)\hat{Q}_o\right] + \frac{\partial}{\partial \eta}\left[\hat{B}_o(\hat{Q}_o)\hat{Q}_o\right] = 0 \tag{111}$$

$$\frac{\partial}{\partial \xi}\left[\hat{A}_o\bar{Q}_1\right] + \frac{\partial}{\partial \eta}\left[\hat{B}_o\,\bar{Q}_1\right] = \frac{\partial}{\partial \xi}\left[\frac{J_1}{J_o}\hat{A}_o\hat{Q}_o\right] + \frac{\partial}{\partial \eta}\left[\frac{J_1}{J_o}\hat{B}_o\hat{Q}_o\right]$$

$$- \frac{\partial}{\partial \xi}\left[\hat{A}_1\hat{Q}_o\right] - \frac{\partial}{\partial \eta}\left[\hat{B}_1\hat{Q}_o\right] \tag{112}$$

It should be noted that

$$\left.\begin{aligned} \hat{A}_1 &= -x_{1x'}\,\xi_{x'}\,\bar{A}_o \\ \hat{B}_1 &= x_1\eta_{x'x'}\,\bar{B}_o \end{aligned}\right\} \tag{113}$$

where $\bar{A}_o$ and $\bar{B}_o$ are cartesian Jacobians and

$$\bar{Q}_1 = \frac{Q_1}{J_o} \tag{114}$$

The boundary conditions for the zeroth approximation, Equation (111), are the same as those for Equation (92).

In the particular formulation of the Euler equations used here a change in freestream Mach number, M_∞, is felt only through the far field boundary condition on ρ and e. For example,

$$\left.\begin{aligned} \rho_\infty &= \frac{1}{\gamma M_\infty^2} \\ e_\infty &= \frac{1}{2} + 1/[\gamma(\gamma - 1)M_\infty^2] \end{aligned}\right\} \tag{115}$$

In order to simplify the algebra a simple test case is chosen. The test case is a flow with a perturbation in freestream Mach number, the geometry remains fixed; this allows the same grid to be used for both the zeroth and first approximations. A second simplification is that the airfoil is symmetric and at zero angle

of attack; this allows the use of symmetrical boundary conditions, thus reducing the computer requirements.

The boundary conditions for the perturbed, primitive variables are therefore as follows.

At the far field boundary

$$\left.\begin{aligned} (\rho u)_1 &= 0 \\ (\rho v)_1 &= 0 \\ e_1 &= \frac{\epsilon}{\gamma(\gamma - 1)M_\infty^2} \\ \rho_1 &= \frac{\epsilon}{\gamma M_\infty^2} \end{aligned}\right\} \qquad (116)$$

where ϵ is a perturbation parameter. The perturbed flow is one where the freestream Mach number, M_1, is given by

$$M_1 = M_\infty/(1 + \epsilon)^{\frac{1}{2}} \qquad (117)$$

On the airfoil surface, denoted by $\eta = 0$, boundary conditions similar to those in Equation (103) are used.

On the symmetry planes the boundary conditions

$$\left.\begin{aligned} \frac{\partial \rho_1}{\partial \xi} &= 0 \\ U_1 &= 0 \\ \frac{\partial V_1}{\partial \xi} &= 0 \\ \frac{\partial e_1}{\partial \xi} &= 0 \end{aligned}\right\} \qquad (118)$$

are used.

For the base solution, Equation (111) is solved using central differencing with added dissipation. This is to ensure that the base solution, Q_o, is smooth except at shock waves. The linear perturbation equation, Equation (112), is solved using central differences with no added dissipation. At the boundaries first order derivatives are approximated by first order differences. Although done mainly for computational use, this has the effect of weakly coupling the odd and even points in the solution. Equation (112) can be written in the discretized form

$$L(Q_1) = B + S \tag{119}$$

where L( ) denotes the difference operator, approximating the left hand side of Equation (112), B denotes the boundary terms applicable to Equation (112) and S denotes the terms due to the straining function. A simplified form of Equation (119) is obtained by neglecting the straining term, S; thus

$$L(Q_1) = B \tag{120}$$

The solutions of Equation (119) or (120) are obtained by direct inversion of the operator L. Thus Equations (119) and (120) become

$$Q_1 = L^{-1}\ (B) + L^{-1}\ (S) \tag{121}$$

and

$$Q_1 = L^{-1}\ (B) \tag{122}$$

respectively. The computations in this analysis are performed on a grid of 40x12 for the half plane. This is the maximum grid size for direct inversions.

The pressure coefficient found from Equation (111) is shown in Figure 10, and it can be seen that it is typical of those seen for transonic flow. The density found from Equation (120) is shown in Figure 17, and it can be seen that it oscillates considerably. This oscillation is typical of central difference approximations when no dissipation is added.

In general a central difference approximation will decouple the odd and even points, and, although the treatment of the boundary conditions allows some coupling between odd and even points, it is instructive to look at a solution composed only of odd or even points. In Figures 18a and 18b the density variation for the odd and even points respectively are shown. It can be seen that the solution in the neighborhood of the sonic line is smooth except for a "spike;" the oscillations near the shock wave are due to the presence of a "nonphysical" sonic line in the shock capture region. Hence, it can be surmised that the same phenomena apparent in the TSD results exists for the "decoupled" linear Euler equations, that is, the solution is smooth except for an oscillatory behavior in the sonic region. In analogy with the TSD result the new shock location is enforced by requiring that the decoupled solutions are smooth at the sonic line. This is accomplished in the same manner as for the TSD equation, namely by enforcing the condition that

$$\frac{\partial^3 Q_1}{\partial \xi^3} = 0 \qquad (123)$$

at the sonic line. Thus, the solution procedure is to solve Equation (121) and determine the parameter δx_s in the term $L^{-1}(S)$ by enforcing Equation (123). The complete solution for Q is determined by

$$Q(x, y) = Q_o(x', y) + \epsilon Q_1 (x', y)$$

5.4 Results

The pressure distribution around a NACA0010 airfoil with $M_\infty = 0.82$ is shown in Figure 19 with a base solution of the same airfoil at $M_\infty = 0.8$. In Figure 19a the odd points are shown, and in Figure 19b the even points are shown. It is not clear why the even points should give a more accurate result than the odd points.

In Figure 20 the pressure distribution around a 10% biconvex airfoil at $M_\infty = 0.828$ is shown with a base solution of the same airfoil at $M_\infty = 0.808$. The odd and even results are shown in Figures 20a and 20b respectively and again it may be observed that the even points give a more accurate result.

There is a general problem with these Euler computations which is the relatively low number of grid points. The maximum number of grid points is determined by the maximum in core storage of the CRAY X MP machine to allow a direct inversion of the operator L( ). It is expected that the grid error in the decoupled points is considerable.

5.5 Concluding Remarks

A linearized form of the Euler equations has been developed and a method of locating shock wave derived. The key to the method is the decoupling of odd and even points and the removal of the characteristic oscillations at the sonic line.

6.) Analysis of the Modeling of Separated Flow Using the Euler Equations

6.1 Introduction

In recent years solutions of the Euler equations have been used to model the flow around aircraft or missiles. The main advantage of the Euler equations over simpler sets of equations

or equations such as the potential equation is that the Euler equations can model nonisentropic, and hence rotational flows. In certain cases, especially missile flows, the ability to capture contact discontinuities and hence model separated flow has been an important feature of the Euler equations. Such flows have several sources of vorticity. Vorticity is generated from curved shock waves and in the viscous boundary layer on bodies. If the boundary layer flow separates from the body, a large vortical region is produced which can be modeled by the Euler equations if the necessary vorticity can be produced. For the Euler equations, vorticity can be produced by curved shocks, by certain boundary conditions, or by numerical discretization error. The numerical error is a somewhat nebulous quantity which seems to be controllable only by careful smoothing and optimization of the computational grid. Boundary conditions for modeling separation usually involve specification of the velocities at or around a specified separation point. If the separation is from missile fins then the separation point is taken to be the fin edges; if body separation is to be modeled then some empirical separation criterion is used to determine the separation point. Also, because of the vorticity generated by curved shocks and numerical error, the Euler equations can have solutions which contain separated flow regions even without the specification of a separation point.

In this section various aspects of modeling separated flows on smooth surfaces using the Euler equations are examined. It is found that "Euler separation" can be radically different in behavior than real, physical separation. It is found also that a separation point cannot be specified arbitrarily on the body without further modification to the Euler equations. It is suggested that numerical treatments of the boundary condition may not be consistent with the Euler equations.

6.2 Analysis

The Euler equations are examined to determine the conditions under which separation is possible in the sense that the flow

tangential to a surface can have a stagnation point. The vorticity equation,

$$U_y - V_x = \omega$$

can be written in terms of a stream function ψ such that

$$\psi_{xx} + \psi_{yy} = \rho\omega + \rho_y U - \rho_x V \tag{124}$$

where ω is the vorticity and

$$\psi_y = \rho U - \rho_\infty U_\infty ; \quad \psi_x = -\rho V \tag{125}$$

The density is given in terms of the entropy, S, and the velocity components U, V by

$$\rho = \rho_\infty \{1 + \frac{(\gamma-1)}{2} M_\infty^2 [1 - U^2 - V^2]\}^{\frac{1}{\gamma-1}} \exp(-S/R) \tag{126}$$

The vorticity is given by Crocco's theorem as

$$\omega = \frac{T}{q} \frac{\partial S}{\partial n} = \frac{p}{R\rho q} \cdot \frac{\partial S}{\partial n} \tag{127}$$

where R is the gas constant

$$q = (U^2 + V^2)^{1/2}$$

and

$$\frac{\partial}{\partial n}$$

is the derivative in the direction normal to the streamlines. Note that

$$\frac{\partial}{\partial n} = U \frac{\partial}{\partial y} - V \frac{\partial}{\partial x} \tag{128}$$

Along a streamline the entropy is constant and hence

$$U \frac{\partial S}{\partial x} + V \frac{\partial S}{\partial y} = 0 \tag{129}$$

The pressure is given by

$$p = p_\infty \{1 + \frac{(\gamma-1)}{2} M_\infty^2 [1 - U^2 - V^2] \}^{\frac{\gamma}{\gamma-1}} \exp(-S/R) \tag{130}$$

Using Equations (126), (127), (128), and (129), Equation (124) can be written as

$$\psi_{xx} = \psi_{yy} = \frac{p_\infty Q^{\gamma/\gamma-1} \exp(-S/R)}{Rq} (U \frac{\partial S}{\partial y} - V \frac{\partial S}{\partial x})$$

$$+ \rho_\infty \frac{\partial}{\partial y} [Q^{\frac{1}{\gamma-1}} \exp(-S/R)] U - \rho_\infty \frac{\partial}{\partial x} [Q^{\frac{1}{\gamma-1}} \exp(-S/R)] V \tag{131}$$

where Q is a function of U and V and is given by

$$Q = [1 + \frac{(\gamma-1)}{2} M_\infty^2 (1 - U^2 - V^2)] \tag{132}$$

Equation (131) can be written as

$$\psi_{xx} + \psi_{yy} = f(x, y) \tag{133}$$

where f(x,y) is the right hand side of Equation (131).

The problem under consideration is the flow around a thin body, given by

$$y = \begin{cases} y_{su}(x) & y \geq 0 \\ y_{sl}(x) & y \leq 0 \end{cases} \tag{134}$$

where the subscripts u and l denote the upper and lower surfaces of the body. The body may be at an angle of attack, α

To some degree of approximation it can be assumed that the body boundary condition can be applied on a slit $y=\pm 0$. The first approximation is thin airfoil theory which gives

$$\left[\frac{(\rho V)}{\rho_\infty U_\infty}\right]_{y=\pm 0} = \begin{Bmatrix} y'_{su}(x) \\ y'_{sl}(x) \end{Bmatrix} - \alpha \tag{135}$$

Equation (133) can be written in integral form using Green's identity to give

$$\int_D \int K(x,\xi;y,\eta) f(\xi,\eta) dD = - \int_{C_1+C_w+C_s+C_\infty} \{K(x,\xi;y,\eta) \frac{\partial \psi}{\partial \nu} (\xi,\eta) - \psi(\xi,\eta) \frac{\partial K(x,\xi;y,\eta)}{\partial \nu}\} dC \tag{136}$$

where C is the boundary of some domain D and ν is the unit inward drawn normal to C. The domain D excludes all regions of the flow where second derivatives of ψ or K do not exist, such as the body (represented by $y = \pm 0$), wakes, shock waves, and contact surfaces. In Equation (136) C_1 is that part of the boundary surrounding the point (x,y), C_w represents the boundary surrounding the x axis, C_s the boundary surrounding the shock waves or contact surfaces and C_∞ is the far field boundary. A sketch of the boundaries C_1, C_w, C_s, C_∞ are shown in Figure 2; to avoid confusion with the entropy, the domain S in Figure 2 is

denoted by D in the present analysis. The kernel function in Equation (136) is given by

$$K(x,\xi;y,\eta) = \frac{1}{2\pi} \ln\{(x-\xi)^2 + (y-\eta)^2\}^{\frac{1}{2}} \tag{137}$$

For subsonic flow the Euler equations are elliptic and hence boundary conditions must be specified on the entire boundary. For transonic flow the flow outside of a finite domain is subsonic so that the same conditions must be satisfied on the outer boundary, C_∞. Equation (136) is similar to the integral equation for potential flow, and it may be deduced (Ref. 6) that the line integral over C_∞ will contribute a finite velocity on C_∞ as $R\to\infty$ if

$$\psi = A \ln R + B \tag{138}$$

where A and B may be functions of the angular coordinate θ.

If this relation is used then the line integral over C_∞ becomes constant.

On performing the various limiting operations as $r\to 0$ and $R\to\infty$ Equation (136) becomes

$$\begin{aligned}\psi(x,y) = {} & \int_0^\infty \{K_o \Delta_o \psi_\eta - K_{o\eta} \Delta_o \psi\} d\xi \\ & - \int_{C_s} \{K_s [\psi_\xi]_-^+ + K_s \frac{\cos(\nu,\eta_s)}{\cos(\nu,\xi_s)} [\psi_\eta]_-^+\} d\eta \\ & + \int_{C_s} [\psi]_-^+ \{\frac{\partial K_s}{\partial \xi} + \frac{\partial K_s}{\partial \eta} \frac{\cos(\nu,\eta_s)}{\cos(\nu,\xi_s)}\} d\eta \\ & + \int_D \int K d\xi d\eta + \text{constant}\end{aligned} \tag{139}$$

where for a function $g(\xi,\eta)$

$$\Delta_o g = g(\xi, +0) - g(\xi, -0) \tag{140}$$

and

$$\left.\begin{aligned} K_o &= K(x,\xi;\ y,o) \\ K_s &= K(x,\xi_s;\ y,\eta) \end{aligned}\right\} \tag{141}$$

ξ_s and η_s are the coordinates of any surface of discontinuity and $\cos(\nu,\eta_s)$, $\cos(\nu,\xi_s)$ are the direction cosines of the normal to these surfaces. $[\ ]_-^+$ denotes a jump across the surface.

If the jumps in derivatives of ψ, such as ψ_x and ψ_y, are finite then ψ must be continuous since a jump in ψ would give an infinite derivative. Hence

$$[\psi]_-^+ = 0 \tag{142}$$

The integrand of the first integral over C_s in Equation (139) becomes

$$K_s\{[\psi_\xi]_-^+ + [\psi_\eta]_-^+ \frac{\cos(\nu,\eta_s)}{\cos(\nu,\xi_s)}\} = [\rho\tilde{q}_t]_-^+ \cos(\nu,\xi_s) \tag{143}$$

where $\tilde{q}_t$ is the velocity tangential to the curve C_s. Hence Equation (139) can be written as

$$\begin{aligned} \psi(x,y) = {} & \int_o^\infty \{K_o \Delta_o \psi_\eta - K_{oy} \Delta_o \psi\} d\xi \\ & - \int_{C_s} K_s [\rho\tilde{q}_t]_-^+ \sec(\nu,\xi_s) d\eta \\ & + \int_D \int K_y f d\xi d\eta + \text{constant} \end{aligned} \tag{144}$$

Equation (144) can be differentiated with respect to y to give

$$\psi_y = \rho U - \rho_\infty U_\infty = \int_o^\infty \{K_{oy}\Delta_o\psi_\eta - K_{o\eta y}\Delta_o\psi\}d\xi$$
$$- \int_{C_s} K_{sy}[\rho\tilde{q}_t]_-^+ \sec(\nu,\xi_s)d\eta$$
$$+ \int_D\int K_y f d\xi d\eta \qquad (145)$$

By integration by parts it can be shown that

$$\int_o^\infty K_{o\eta y}\Delta_o\psi d\xi = \int_o^\infty K_{ox}\Delta_o\psi_\xi d\xi \qquad (146)$$

$$\int_D\int K_y f d\xi d\eta = \int_o^\infty K_{oy}\Delta_o F d\xi - \int_D\int K_{y\eta} F d\xi d\eta \qquad (147)$$

where

$$F = \int^\eta f(\xi,\eta')d\eta' \qquad (148)$$

Thus Equation (145) can be written as

$$\rho U - \rho_\infty U_\infty = - \int_o^\infty K_{ox}\Delta_o\psi_\xi d\xi + \int_o^\infty K_{oy}[\Delta_o\psi_\eta - \Delta_o F]d\xi$$
$$- \int_{C_s} K_{sy}[\rho\tilde{q}_t]_-^+ \sec(\nu,\xi_s)d\eta$$
$$- \int_D\int K_{y\eta} F d\xi d\eta \qquad (149)$$

On differentiation of Equation (144) with respect to x and performing a similar integration by parts

$$\rho V = - \int_o^\infty K_{ox}\{\Delta_o\psi_\eta - \Delta_o F\}d\xi + \int_o^\infty K_{oy}\,\Delta_o\psi_\eta\,d\xi$$

$$- \int_{C_s} K_{sx}[\rho\tilde{q}_t]_-^+ \sec(\nu,\xi_s)d\eta$$

$$- \int_D\int K_{x\eta}Fd\xi d\eta \qquad (150)$$

If the limit as $y \to \pm o$ is taken of Equations (149) and (150) the following equations result

$$[(\rho U)_{y = \pm 0}]^{\mp} \Delta_o\frac{(\rho U)}{2} - \rho_\infty U_\infty = - \int_o^\infty \frac{\Delta_o\psi_\xi d\xi}{x-\xi}$$

$$- \lim_{y\to\pm o} \{ \int_D\int K_{y\eta}[F(\xi,\eta) - F(x,\pm o)]d\xi d\eta$$

$$- \int_{C_s} K_{sy}[\rho\tilde{q}_t]_-^+ \sec(\nu,\xi_s)d\eta\} \qquad (151)$$

$$- \{(\rho V)_{y = \pm o}^{\mp} \frac{\Delta_o(\rho V)}{2} \} = \int_o^\infty \frac{[\Delta_o(\rho U)-\Delta_o F]}{x - \xi}d\xi$$

$$+ \lim_{y\to\pm o} \{-\int_{C_s} K_{sx}[\rho\hat{q}_t]_-^+ \sec(\nu,\xi_s)d\eta$$

$$- \int_D\int K_{x\eta}Fd\xi d\eta\} \qquad (152)$$

It can be seen then that on $y = \pm o$ Equation (149) gives only the symmetric part of ρU; the asymmetric part is given by Equation (152) in terms of the symmetric part of $(\rho V)_{y = o}$.

It should be noted that in both Equation (149) and Equation (150) the integral over C_s may contribute a discontinuity depending on the orientation of C_s to the axis. For example, if C_s is in the direction of the y axis (a normal shock wave perhaps) the integral over C_s in Equation (149) is continuous. Since the other integrals are continuous (Ref. 6), ρU is continuous through a normal shock; this is the correct Rankine-Hugoniot solution. However, in Equation (150) the integral over C_s provides the term

$$- \frac{1}{2} [\rho V]^{+}_{-} \mathrm{sgn}(x_s - x)$$

where x_s is the location of the shock. This term ensures that Equation (150) is consistent on both sides of the shock. The actual value of $[\rho V]^{+}_{-}$ can be found from the jump relations, either for a shock wave or a contact discontinuity.

From Equations (126) and (131) it can be seen that ρ and f (and consequently F) are functions only of U and V and the entropy S. The entropy is given by Equation (129) and the velocities just ahead of the shock wave. Thus S is a function only of U, V. Hence, if $(\rho V)_y = \pm o$ is defined as a boundary condition Equations (149) and (150) are equations for U and V throughout the flow field. Because of the complexity of the relations for ρ,S and F it is not easy to determine the number of possible solutions. However, it is safe to say that if ρV is specified on the body then ρU and ρV are determined completely in the flow field; ρU is also determined on the body. In otherwords, U and V cannot both be specified on the boundary; this statement requires further discussion.

It has been the practice in some problems to model separated flow using the Euler equations. In these methods an empirically determined separation line is specified. The separation line is such that the flow on at least one side of the resulting contact surface on the body surface is a stagnation point. In effect the method is specifying both U and V at this point and from the above argument this overspecifies the boundary conditions for the Euler equations. The necessary additional degree of freedom for these techniques could be introduced by an additional entropy or vorticity source which would mimic the absent boundary layer generated vorticity.

A second point that arises is the use of extrapolation of the tangential velocity to get a value on the surface, for example, by the use of boundary conditions of the type in

Equation (103). These conditions specify the tangential velocity on the surface in contradiction to the above argument. Consequently, solutions employing this device are not solutions of the Euler equations, although the error is difficult to estimate, and the approximation may be adequate in an engineering sense.

The asymmetric or "lifting" part of ρU is given by Equation (152). This equation is similar to one in classic aerodynamic theory and has at least one eigensolution such that Equation (152) can be written as

$$- \{(\rho V)_{y=\pm o} \mp \frac{\Delta_o(\rho V)}{2}\} = \int_o^\infty \frac{[\Delta_o(\rho U) - \Delta_o F - AG(\xi)]}{x - \xi} d\xi + \lim_{y \to \pm o} \{-\int_{c_s} K_{sx} [\rho \tilde{q}_t]_-^+ \sec(\nu, \xi_s) d\eta - \int_D \int K_{x\eta} F d\xi d\eta\} \quad (153)$$

where

$$G(\xi) = \begin{cases} 1/[\xi\ (1 - \xi)\ ]^{\frac{1}{2}}; & \xi \leq 1 \\ o \qquad\qquad\quad ; & \xi \geq 1 \end{cases} \quad (154)$$

and A is an arbitrary constant. An additional condition is necessary to determine the constant. A general solution of Equation (153) is

$$\Delta_o(\rho U) - \Delta_o F = AG(x) + H(x) \quad (155)$$

where H(x) is the "basic" solution. Since any choice of A other than zero would make $(\Delta_o(\rho U) - \Delta_o F]$ infinite at the trailing edge the logical choice is

$$A = 0 \tag{156}$$

It is important to note that this condition, the classic Kutta condition, must be imposed either explictly or implicitly in any solution procedure since, in general, the Euler equations can give an arbitrary lift.

As a final point it can be stated that if a separation point in the Euler equations is defined as a stagnation point, then for a symmetric body Equation (151) can conceivably give a solution that will make U zero at some point on the surface. The actual point is determined by the body geometry and by the entropy generated in the flow. For a lifting flow a similar situation arises but some measure of control on the location of the separation points is given by the arbitrary constant, A, discussed above.

6.3 Additional Comments on "Euler" Separation

One of the jump conditions across a vortex sheet is that

$$\Delta p = 0 \tag{157}$$

Equations (130) and (157) then give

$$\{1 + \frac{(\gamma-1)}{2} M_\infty^2 [1 - q^{+2}]\} \exp(-S^+/c_p)$$

$$= \{1 + \frac{(\gamma-1)}{2} M_\infty^2 [1 - q^{-2}]\} \exp(-S^-/c_p) \tag{158}$$

where "+" and "-" signs denote values on the upstream and downstream sides of the separation point respectively.

If the velocity on the downstream side is zero, then Equation (158) gives

$$q^{+2} = - \frac{2}{(\gamma-1)\ M_\infty^2} \{[1 + \frac{(\gamma-1)}{2} M_\infty^2] [\exp(\Delta S/c_p) -1]\} \quad (159)$$

where

$$\Delta S = S^+ - S^- \quad (160)$$

For a real value of q+ to exist

$$\exp(\Delta S/c_p) \leq 1 \quad (161)$$

For ΔS equal to zero, that is isentropic flow,

$$q^+ = 0 \quad (162)$$

In other words, if separation occurs in isentropic flow, the flow has a stagnation point at both sides of the separation.

From Equation (161)

$$S^+ \leq S^- \quad (163)$$

If a shock wave is upstream of the separation and produces entropy then Equation (163) cannot be satisfied. Re-examining Equation (158), it is found that this implies that at the separation point the stagnation point should be on the upstream side of the separation point, in other words the separation streamline would be inclined in the upstream direction. This flow feature does not appear in experiment thus indicating some of the peculiarities of separation phenomena in the Euler equations.

Since the flow is attached before separation it follows that for a convex surface

$$\frac{\partial p}{\partial n} > 0 \tag{164}$$

where n is the direction normal to the surface.

Using Equation (130), Equation (164) becomes

$$-\gamma M_\infty^2 q \frac{\partial q}{\partial n} - \{1 + \frac{(\gamma-1)}{2} M_\infty^2 (1-q^2)\} \frac{\partial}{\partial n} (S/R) \geq 0 \tag{165}$$

or

$$\frac{\partial q}{\partial n} < - (\frac{1}{\gamma M_\infty^2 q}) \{1 + \frac{(\gamma-1)}{2} M_\infty^2 (1-q^2)\} \frac{\partial}{\partial n} (S/R) \tag{166}$$

If the flow is isentropic then $\partial q/\partial n$ is negative in contradiction to $\partial q/\partial n$ for a viscous flow which is positive. However, if $\partial(S/R)/\partial n$ is negative, as it will be for a shock generated entropy, $\partial q/\partial n$ will be positive and have the same sign as for a viscous flow, thus giving some realism to the flow model.

Separation is characterized by the vorticity in the boundary layer. For a turbulent boundary layer an approximation to the vorticity is given by

$$\omega_b \simeq \frac{\partial q}{\partial n} \simeq q_e \frac{\partial}{\partial n} (\frac{n}{\delta})^{\frac{1}{7}} = \frac{q_e}{7\delta} (\frac{n}{\delta})^{-6/7} \tag{167}$$

where ω_b is the vorticity due to the boundary layer, δ is the boundary layer thickness, and q_e is the velocity external to the boundary layer. From Equation (167)

$$\omega_b \geq \frac{q_e}{7\delta} \tag{168}$$

The vorticity generated by the shock wave is given by Crocco's theorem, Equation (129), and can be written as

$$\omega_E = \frac{1}{\gamma} \frac{a^2}{q} \frac{\partial(S/R)}{\partial n} \tag{169}$$

where ω_e is the vorticity generated by the shock wave and a is the speed of sound. Hence,

$$\frac{\omega_E}{\omega_b} \leq \frac{7\ \delta}{\gamma q_e^2}\ a^2\ \frac{\partial(S/R)}{\partial n} = \frac{7\ \delta}{\gamma M^2} \frac{\partial}{\partial n}\ (S/R) \tag{170}$$

where M is the local Mach number for the Euler calculation and q has been identified with q_e.

The entropy rise through a weak shock is given approximately by (Ref. 7)

$$\frac{\partial(S/R)}{\partial n}\bigg|_{shock} \simeq \frac{4\gamma}{(\gamma+1)^2}\ (M_1^2 - 1)^2 M_1\ \frac{\partial M_1}{\partial n} \tag{171}$$

where M_1 is the Mach number just ahead of the shock. If it is assumed that

$$\frac{\partial}{\partial n}\ (S/R) \simeq C\ \frac{\partial}{\partial n}\ (S/R)\bigg|_{shock} \tag{172}$$

then Equation (170) gives

$$\frac{\omega_E}{\omega_b} \leq \frac{7\ C\ \delta}{\gamma\ M^2} \cdot \frac{4\gamma}{(\gamma+1)^2}\ (M_1^2 - 1)^2 M_1 \left|\frac{\partial M_1}{\partial n}\right|_{shock} = F \tag{173}$$

This equation indicates that the vorticity generated by the shock is much less than that generated by the boundary layer for weak shocks but that as M_1 increases, the inviscidly generated vorticity can dominate.

A crude indication of the magnitude of ω_E/ω_b is given as follows: Let C be unity, M $\simeq$ 1, δ = 0.01, (the boundary layer thickness). Finally, assume the shock length is unity and that the variation of M_1 along the shock is linear. Hence,

$$\frac{\partial M_1}{\partial n} \simeq -(M_1 - 1) \tag{174}$$

The variation of the function F with M_1 is shown in Table 1.

M_1	F
1.0	0
1.2	0.0023
1.4	0.0251
1.6	0.1136
1.8	0.3512
2.0	0.8750
2.2	1.8924
2.4	3.7007
2.6	6.7092

Table 1

It can be seen that the overall contribution of the shock generated vorticity increases rapidly with the strength of the shock, indicating that at the higher supersonic Mach numbers the vorticity field is dominated by the shock induced vorticity.

7.) Concluding Remarks

This work is concerned with developing methods for solving transonic flow problems using linearized forms of the TSD equation and the Euler equations. Methods have been developed using both integral equation methods and finite difference methods. A key element in both the TSD and Euler models is the use of a strained coordinate system in which the shock remains fixed. Additional criteria are then developed to determine the free parameters in the coordinate straining; these free parameters are functions of the shock location.

From an integral equation analysis it is found that the shock wave is located by ensuring that no expansion shocks exist in the solution. If a numerical solution is obtained, this expansion shock is represented by oscillations in the solution near the sonic line; the correct shock location is determined by removing these oscillations. In other words, the oscillations are a crucial element in locating the shock wave. This conclusion is true for finite difference solutions as well as integral equation solutions. Finite difference algorithms frequently have dissipation to remove oscillations caused by numerical error at shock waves. It is shown in the present work that such algorithms can remove the oscillations at the sonic line, thus eliminating the mechanism for locating the shock wave. An example is given of a plausible result which has the shock in the wrong location. The important point is that algorithms should reflect the mathematics of the equations. Since in many cases the mathematics are unknown, it is possible that commonly used algorithms could lead to nonphysical results.

A second, major, study is that into the ability of the Euler equations to model separated flow. The investigation shows that the correct boundary condition is that velocity normal to the solid body should be zero; all other flow variables can be obtained from the resulting equation. Thus it is not consistent to specify a separation point on the body since this imposes an inconsistent value of the tangential velocity. The one exception to this statement is for a lifting case where a Kutta condition, which imposes a separation point, is necessary to close the solution. As a final point, it is shown that "Euler separation" does have some nonphysical features. Again, it must be stressed that more study of the mathematical nature of the Euler equations is necessary to prevent the use of algorithms that are inconsistent with the differential equations.

REFERENCES

1. Jameson, A. and Baker T. J.: Solution of the Euler Equations for Complex Configurations. AIAA Paper 83-1929, 1983.

2. Nixon, D. and Liu, Y.: Concepts for Radically Increasing the Numerical Convergence Rate of the Euler Equations. Nielsen Engineering & Research, Inc. Report 326, 1984.

3. Nixon, D.: Perturbation of a Discontinuous Transonic Flow. AIAA Journal, Vol. 16, No. 1, 1978.

4. Nixon, D.: Calculation of Unsteady Transonic Flow Using an Integral Equation Method. AIAA Journal, Vol. 16, No. 9, 1978.

5. Stahara, S. S.: Operational Manual for Two-Dimensional Transonic Code TSFOIL. NASA CR 3064, 1978.

6. Nixon D.: Calculation of Transonic Flows Using Integral Equation Methods. Ph.D. Thesis, University of London, 1976.

7. Liepmann, H. and Roshko, A.: Elements of Gas Dynamics, Wiley, 1957.

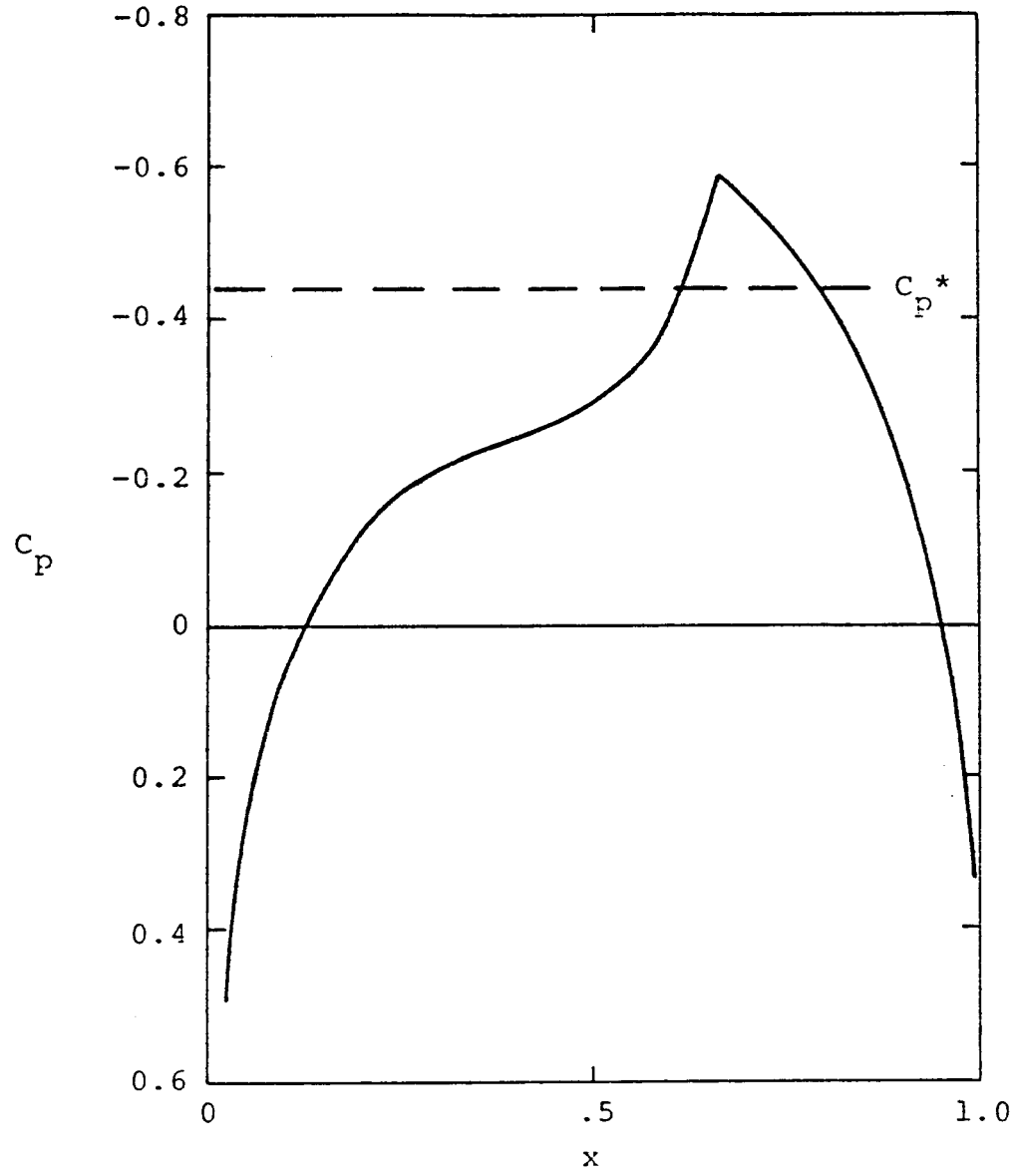

Figure 1.- Pressure distribution for the Linearized TSD Equation (TSFOIL).

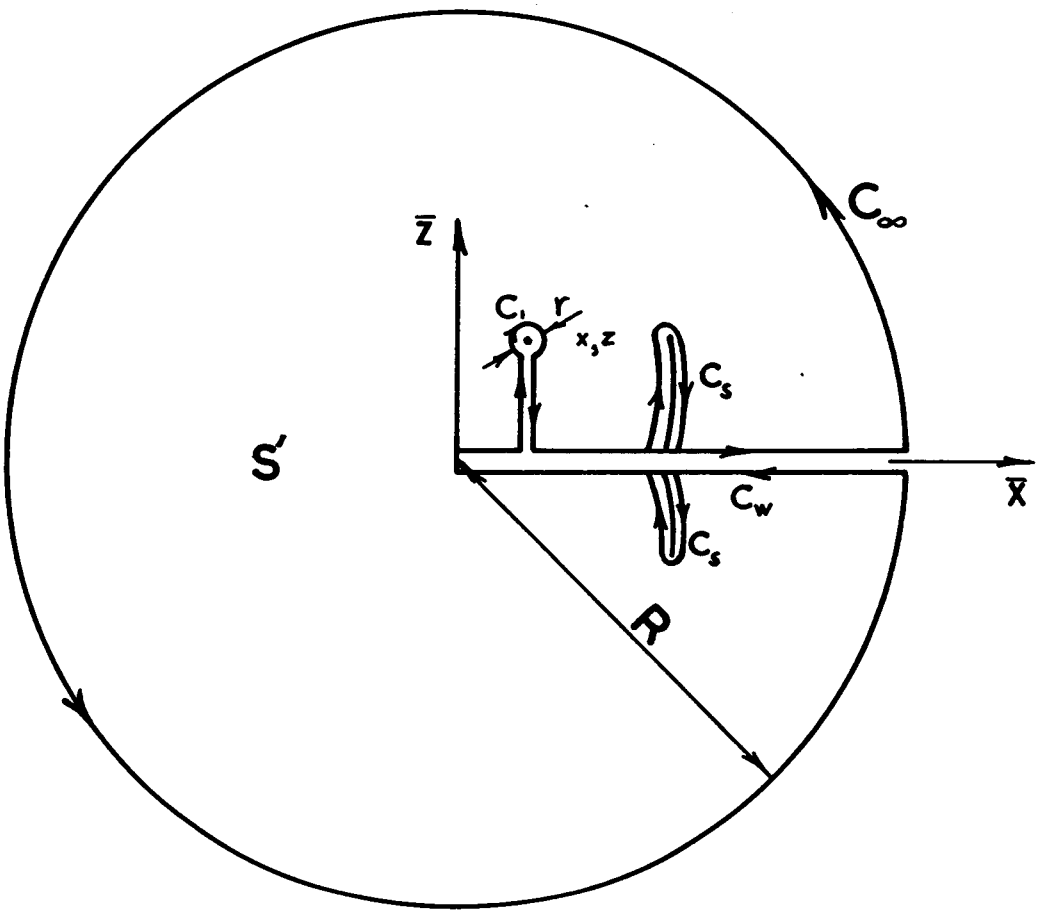

Figure 2.- Domain of Integration for Greens Theorem.

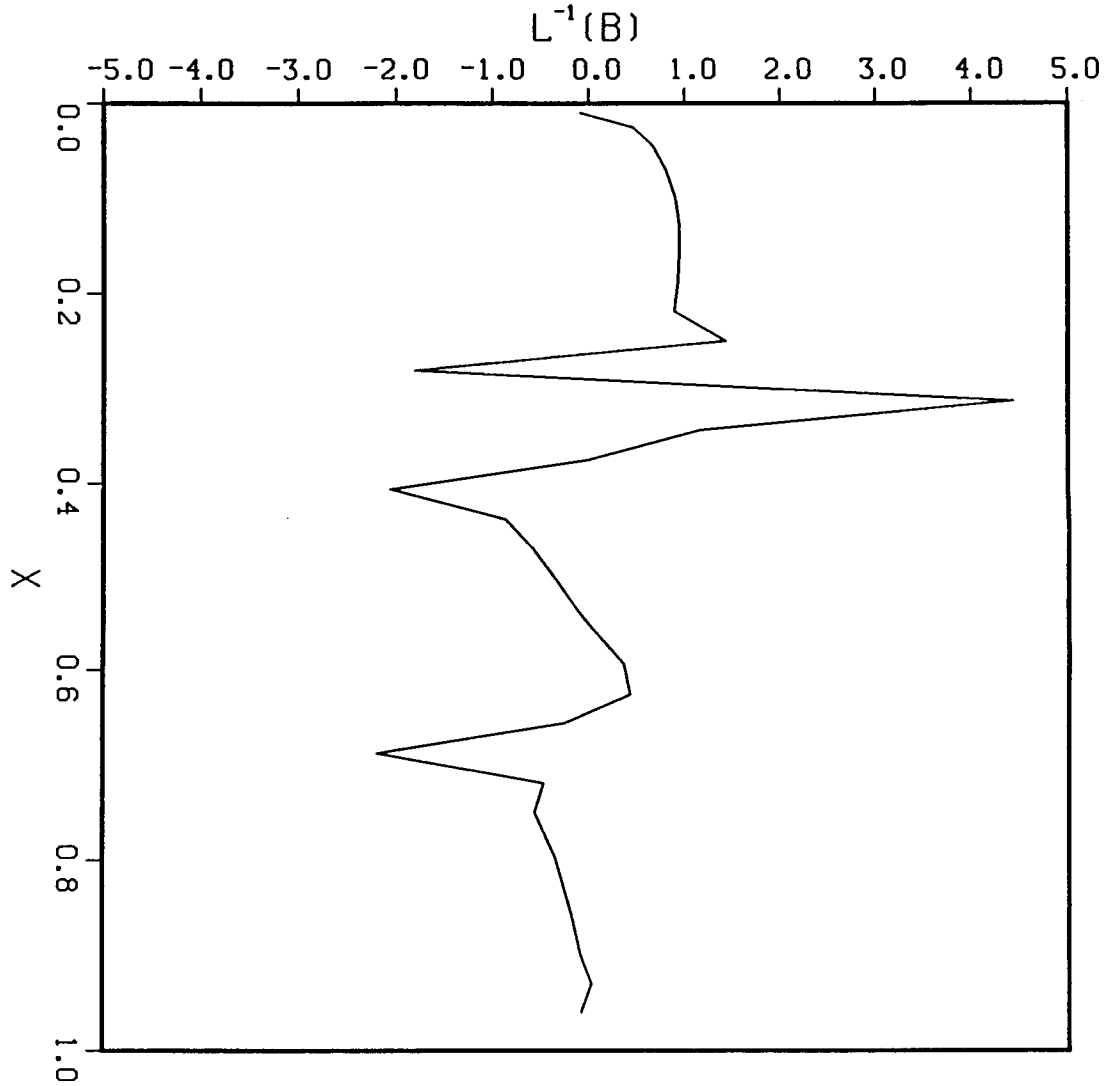

Figure 3.- Solution of Integral Equation with No Straining.

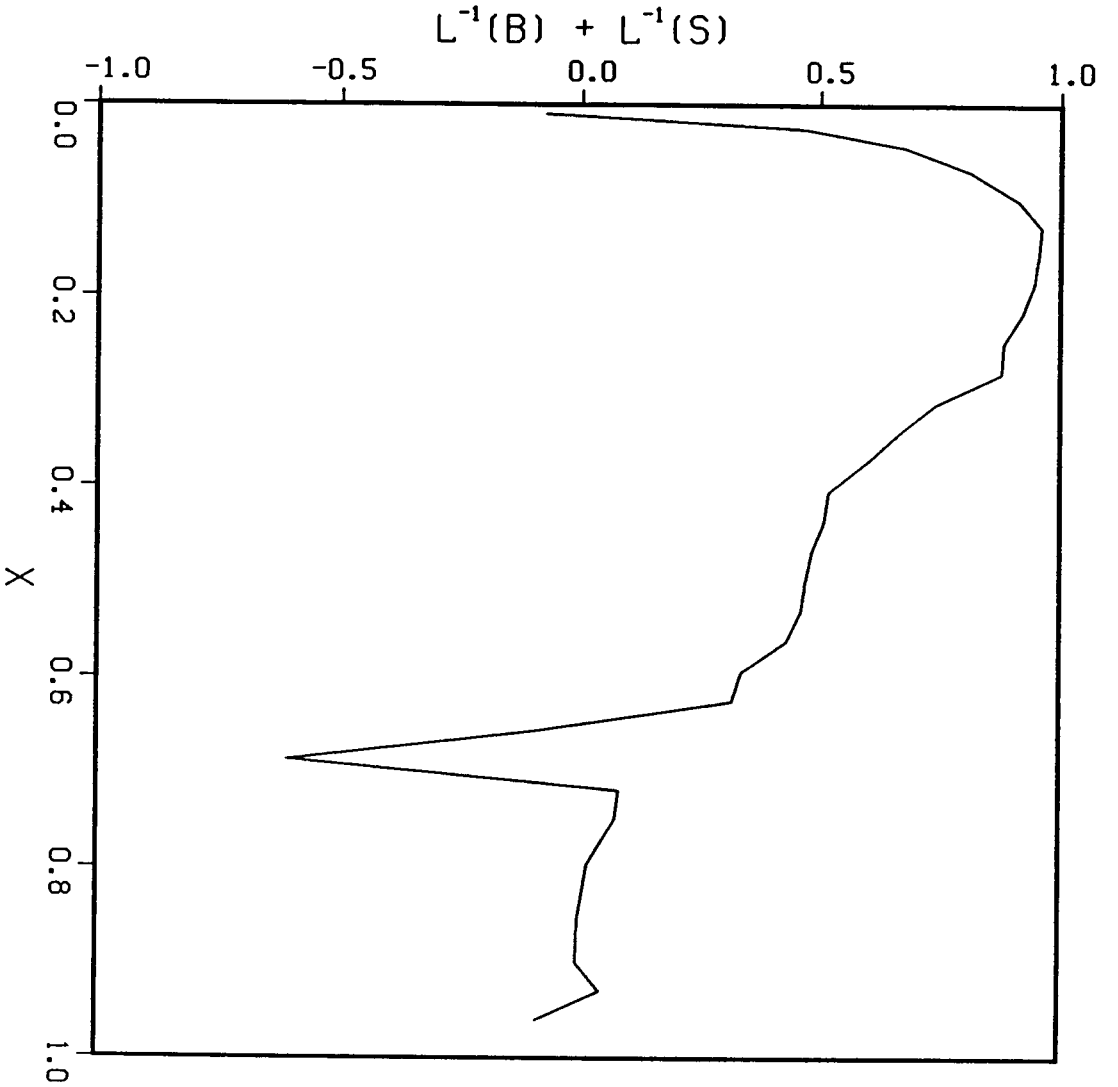

Figure 4.- Solution of Integral Equation.

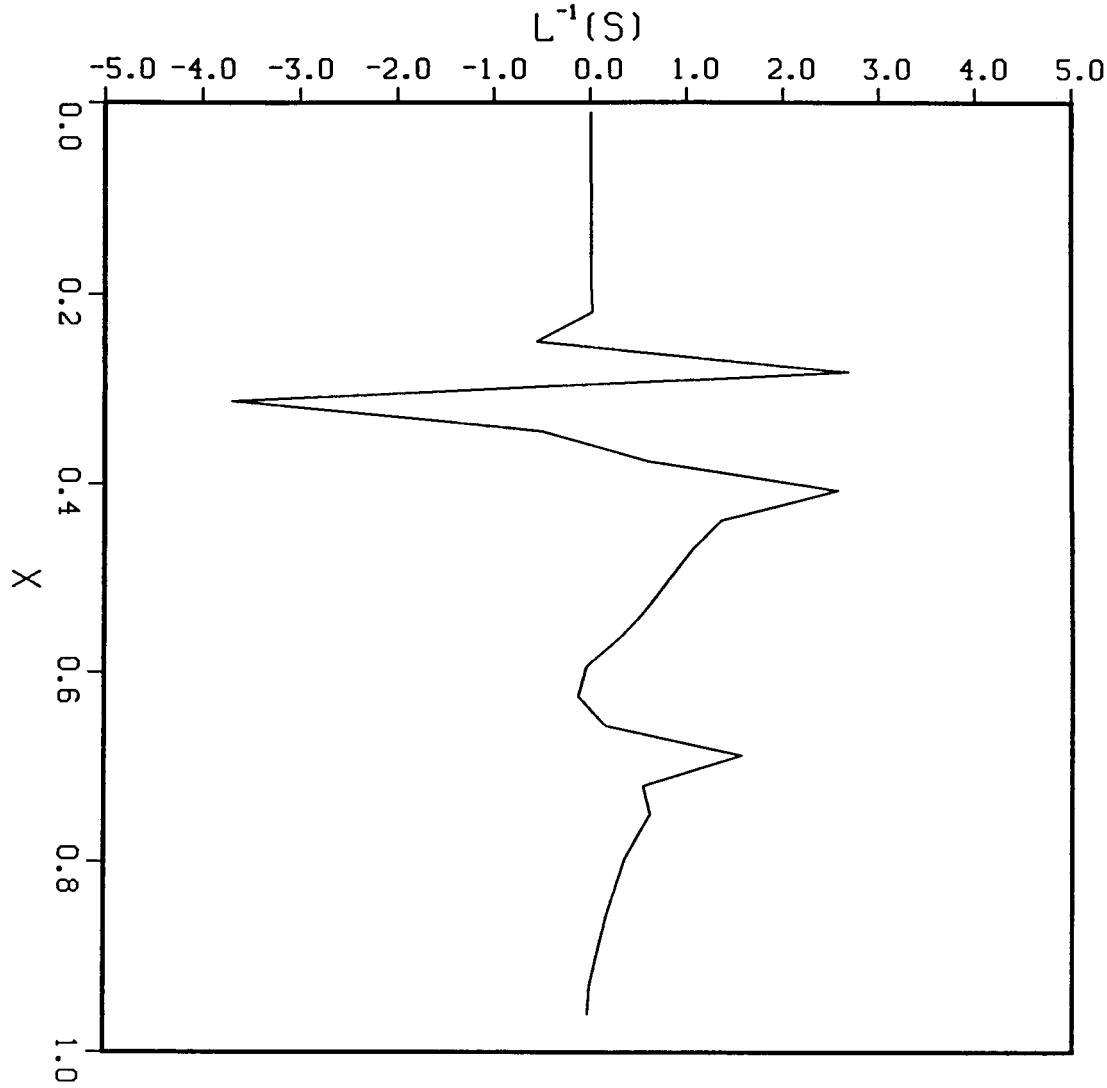

Figure 5.- Straining Term for Integral Equation.

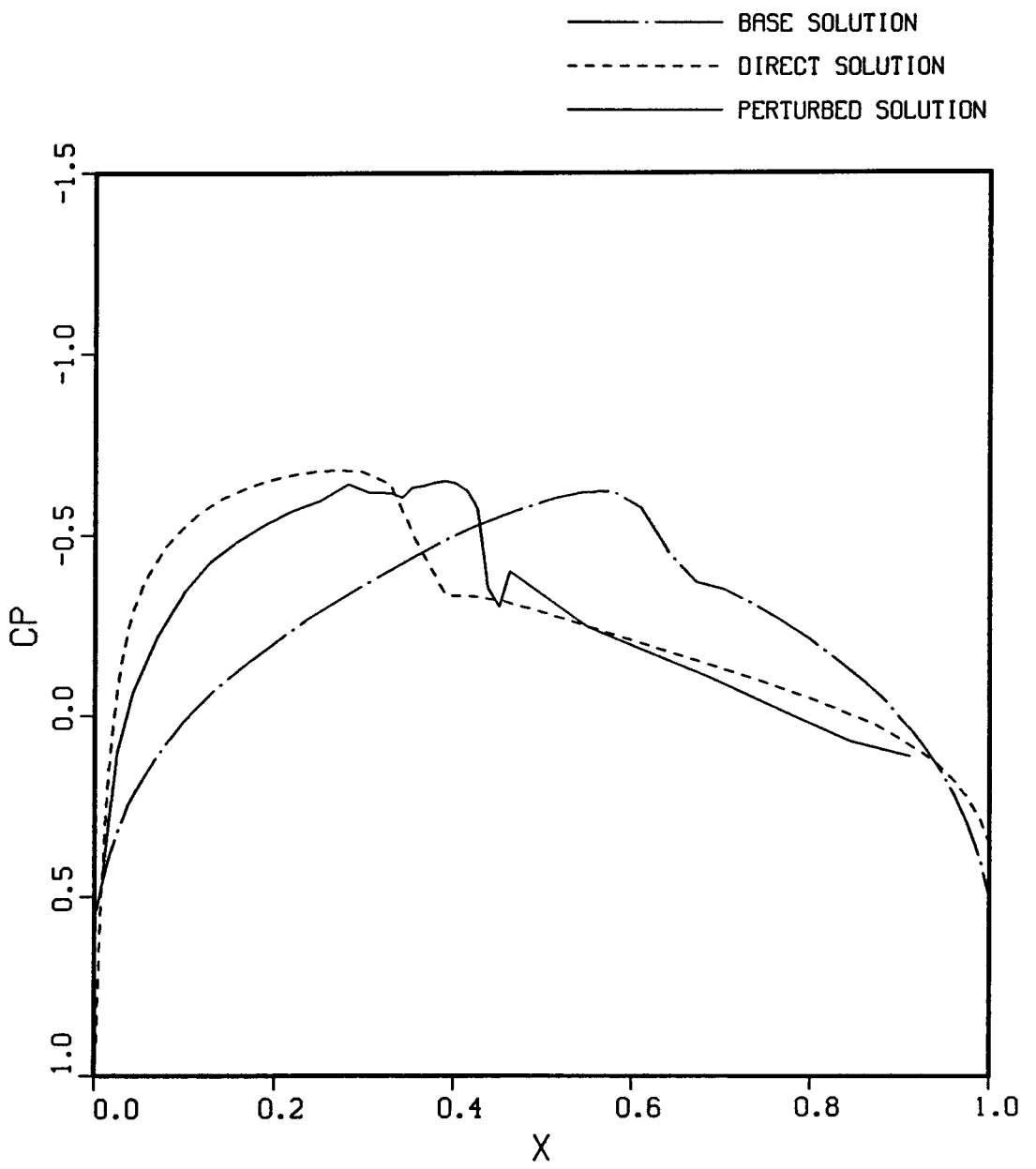

Figure 6.- Pressure Distribution Around a NACA0010 Airfoil, $M_\infty = 0.808$

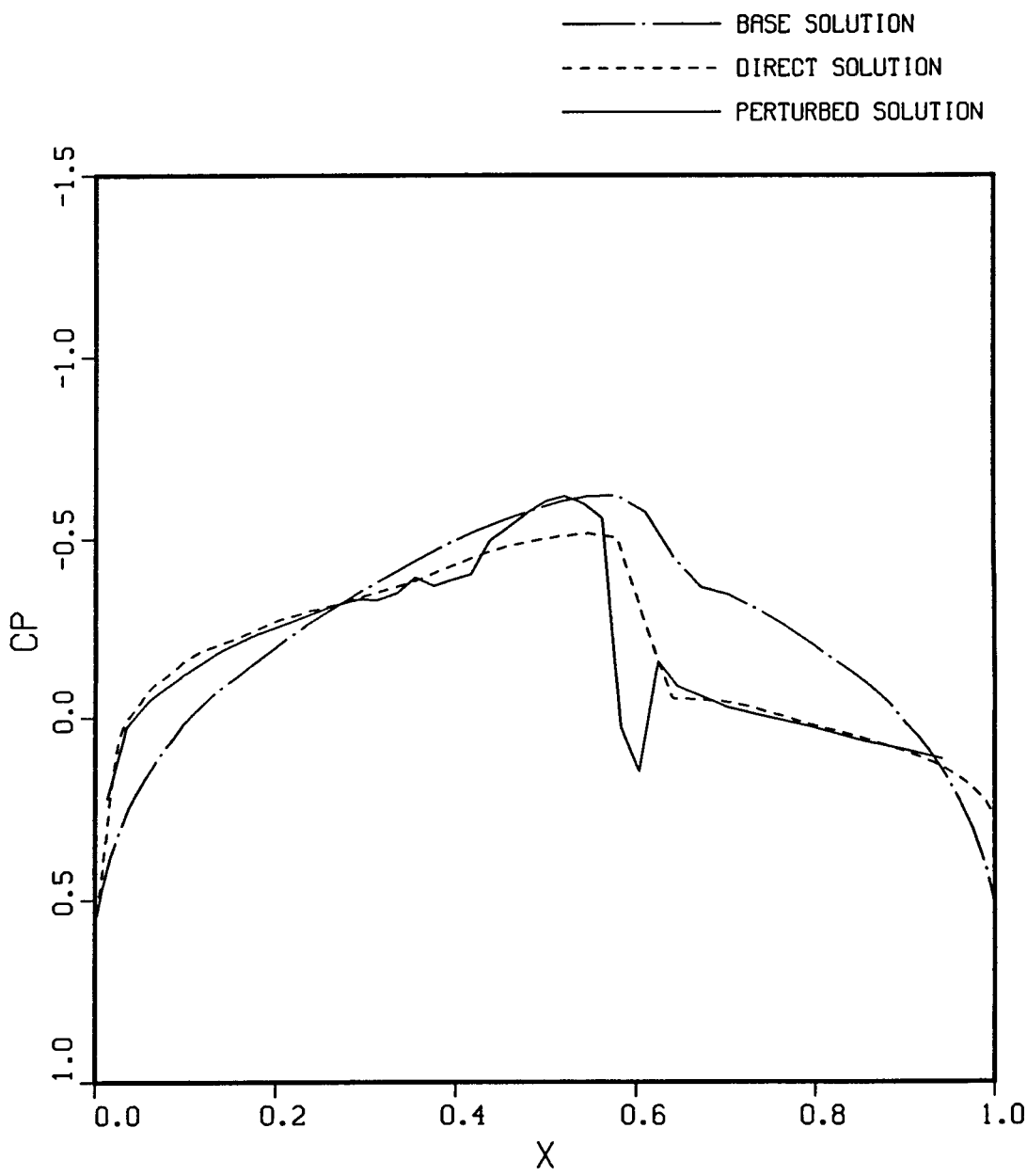

Figure 7.- Pressure Distribution Around a NACA 64A006 Airfoil, $M_\infty = 0.875$

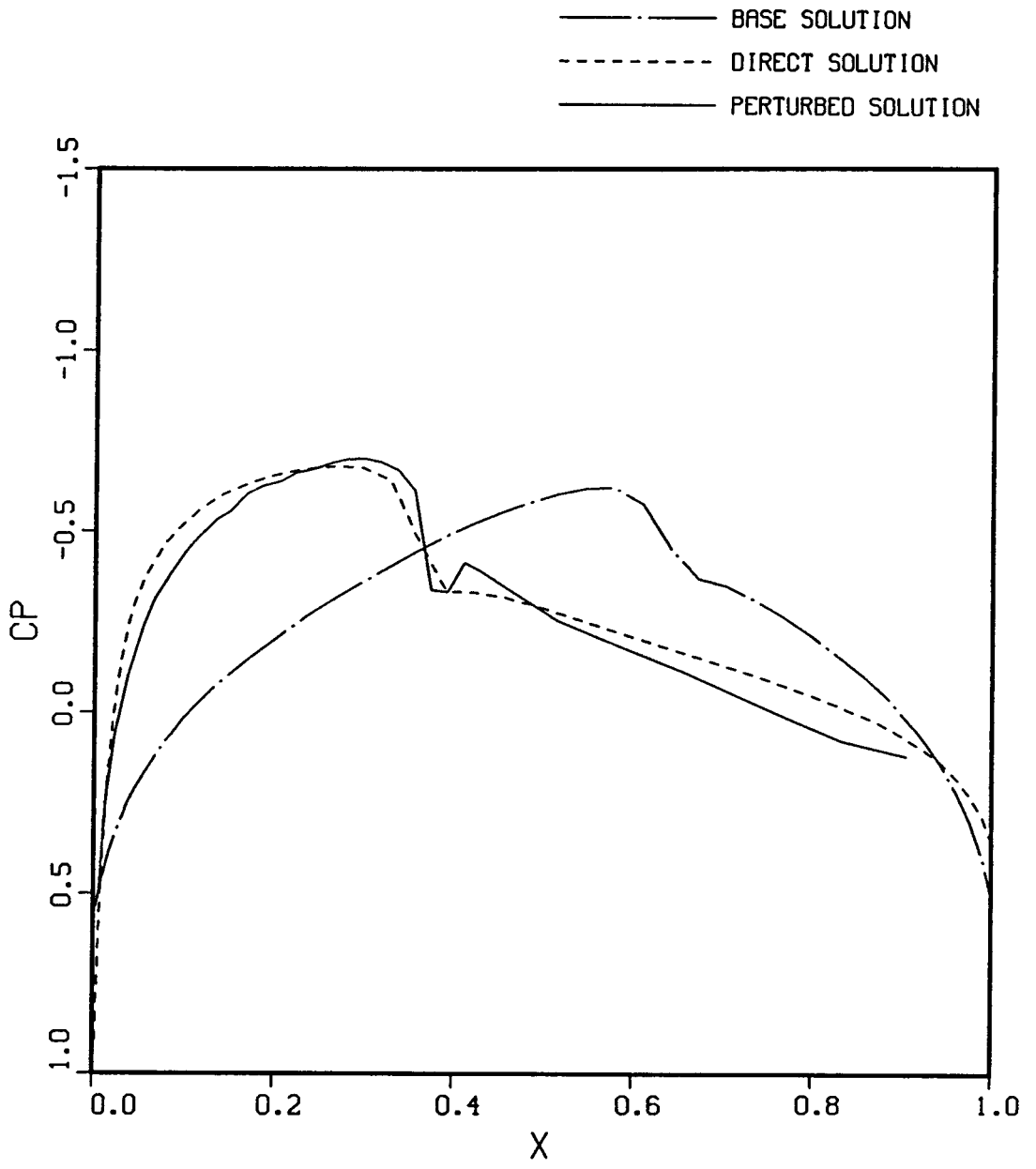

Figure 8.- Pressure Distribution Around a NACA 0010 Airfoil; M_∞ = 0.808 with Double Straining.

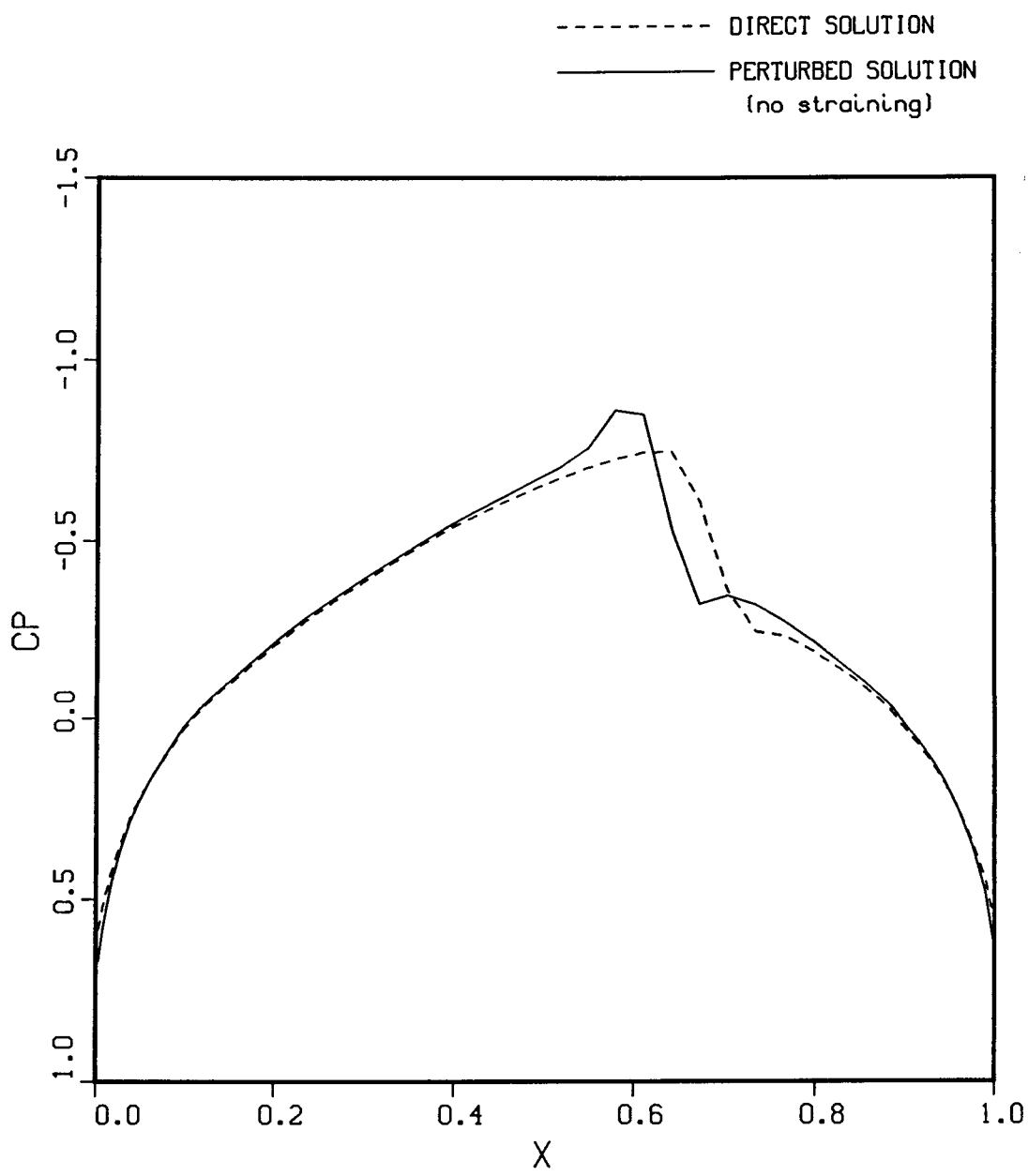

Figure 9.- Finite Difference Solution with Mixed Differences.

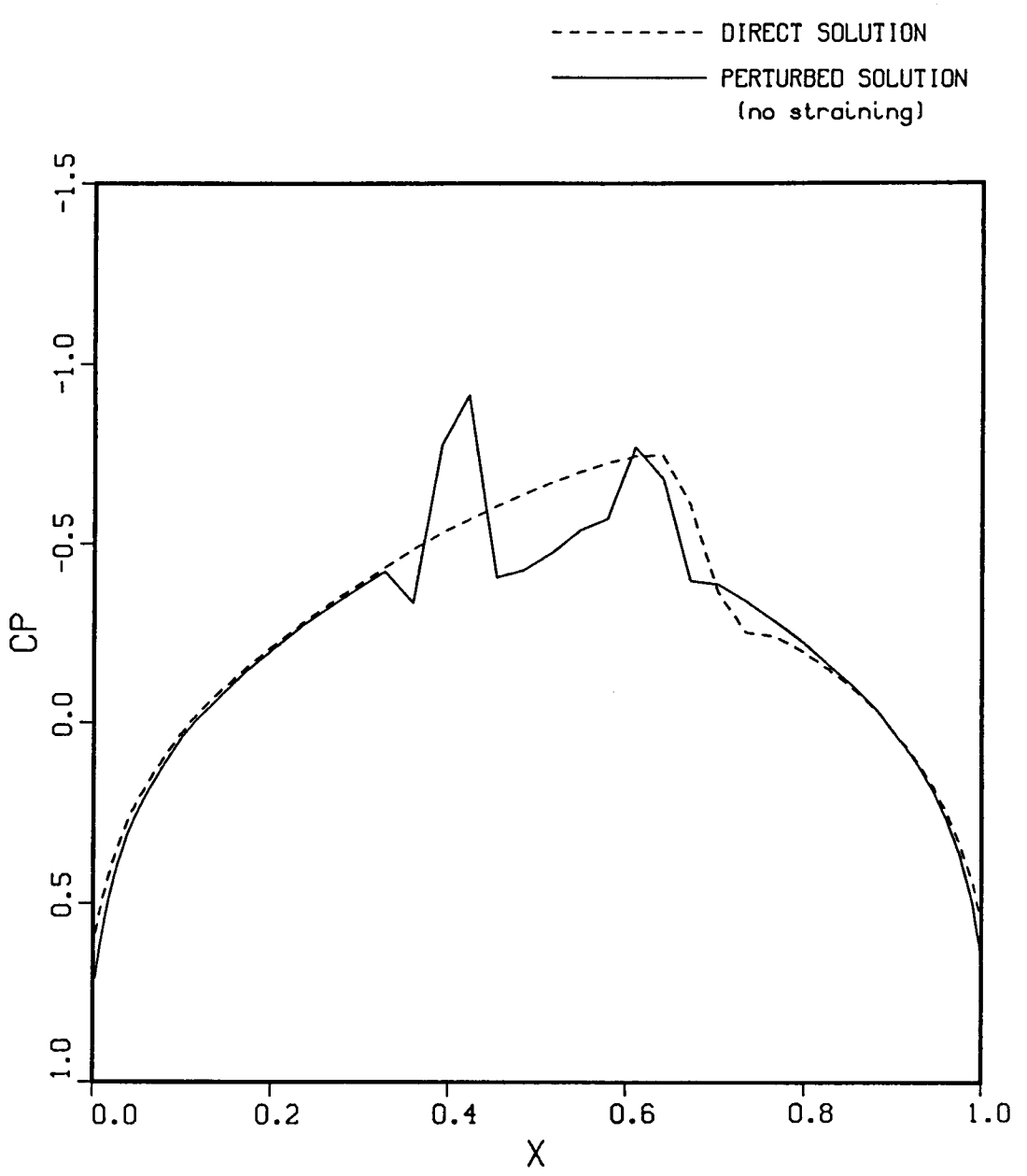

Figure 10.- Finite Difference Solution with Central Differences (11% biconvex airfoil).

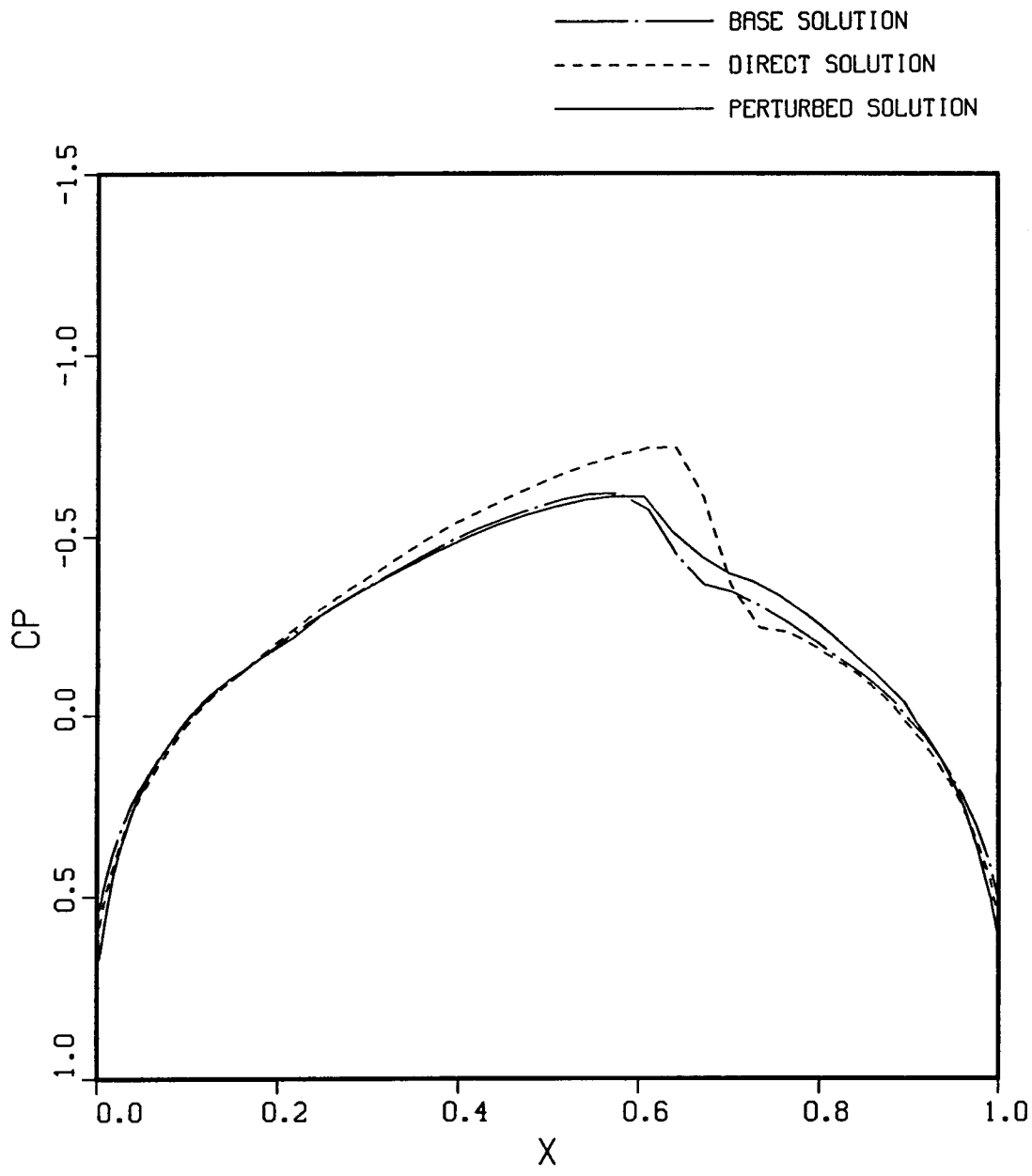

Figure 11.- Finite difference Solution with Coordinate Straining (11% biconvex airfoil).

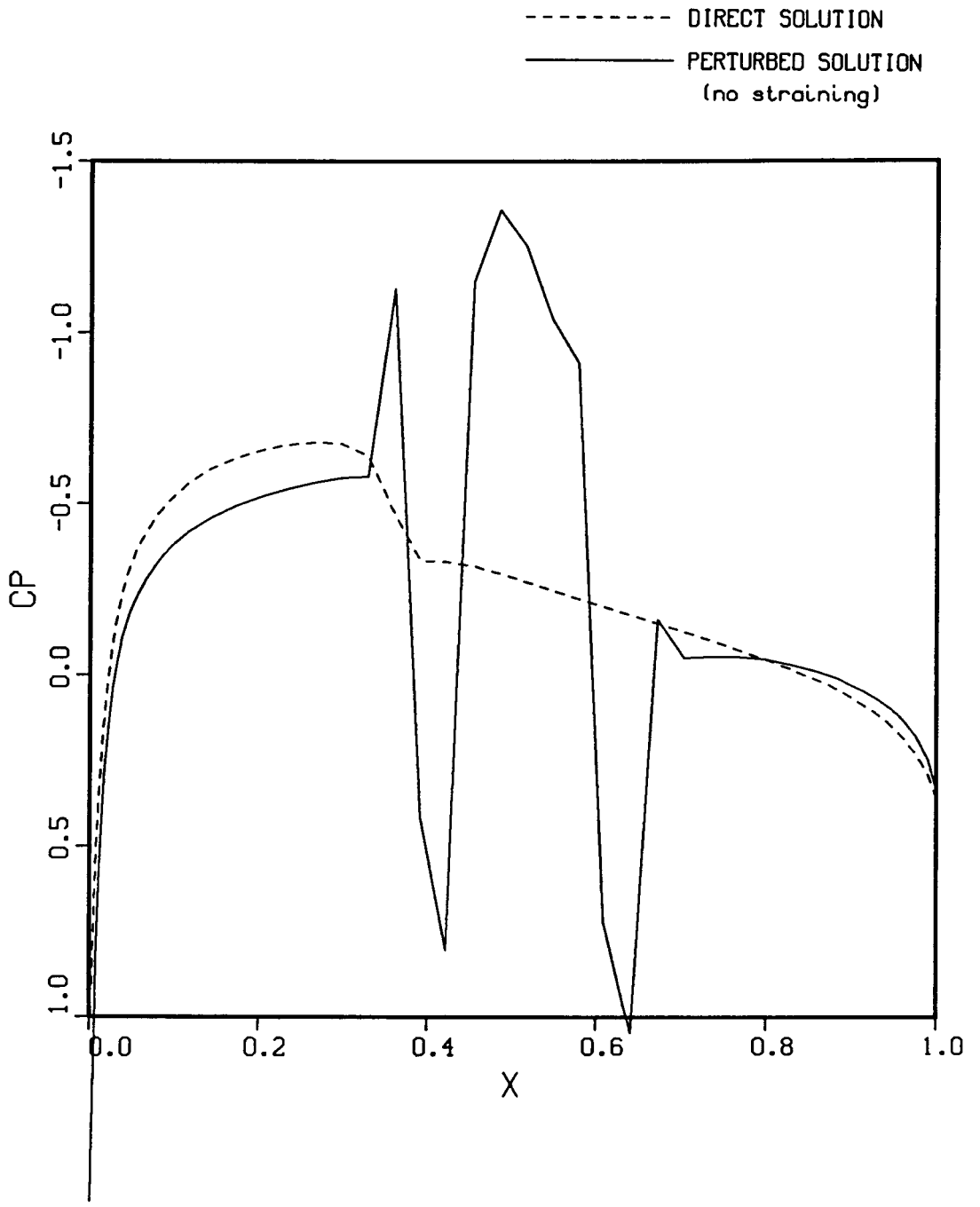

Figure 12.- Finite Difference Solution with Central Differences (NACA 0010 airfoil).

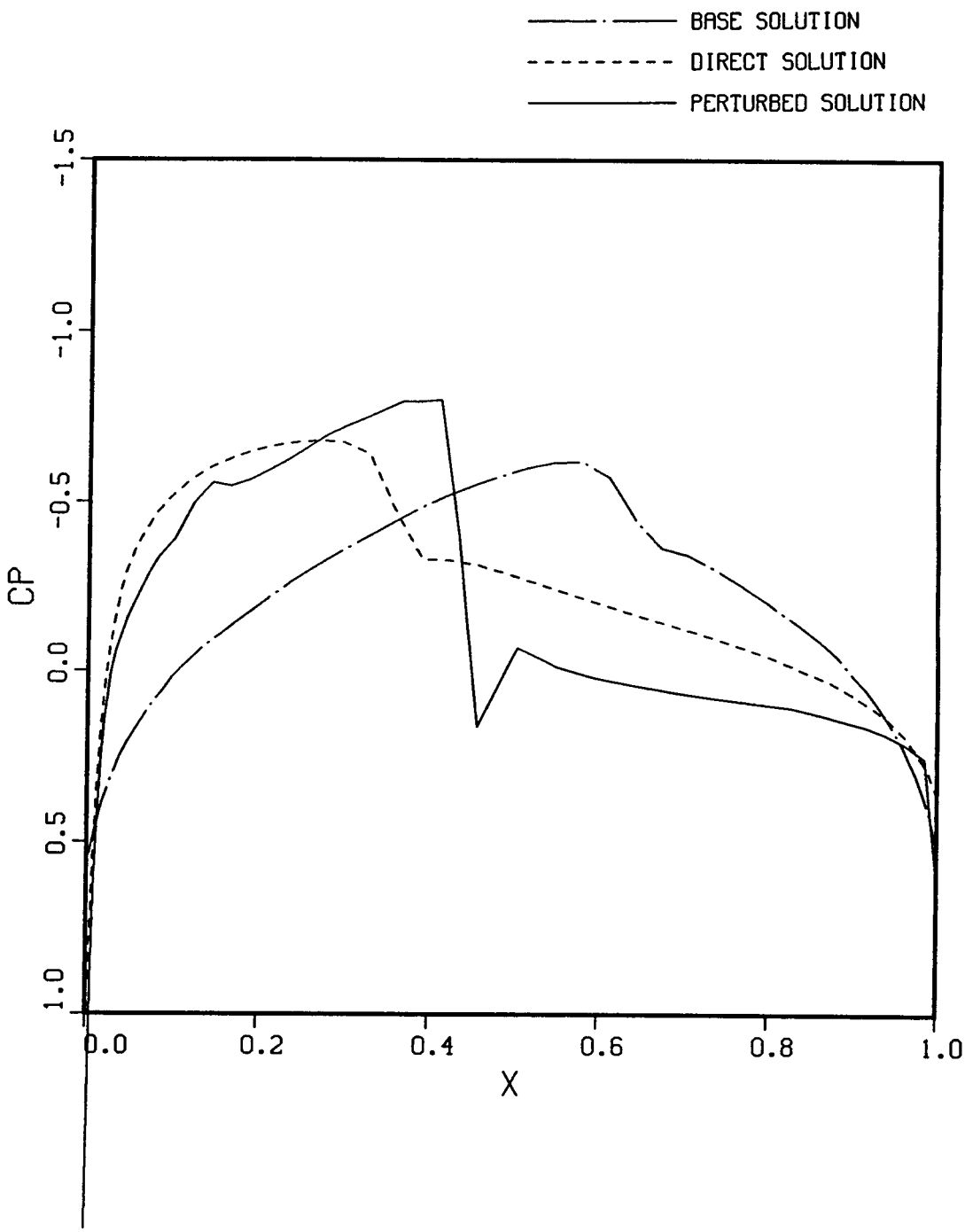

Figure 13.- Finite Difference Solution with Coordinate Straining (NACA 0010 Airfoil).

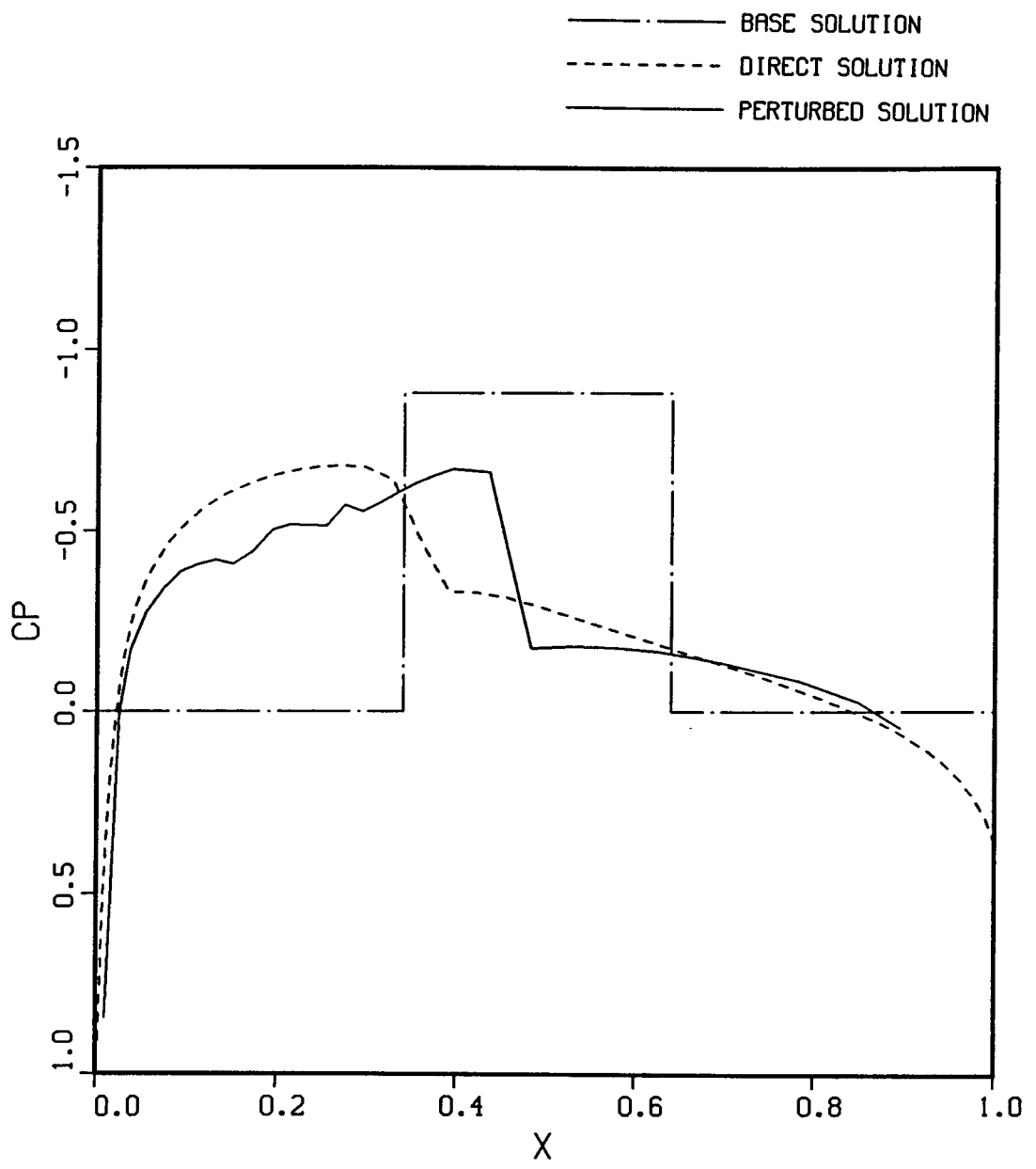

Figure 14.- Solution of Linear Constant Coefficient Equation (NACA 0010 Airfoil).

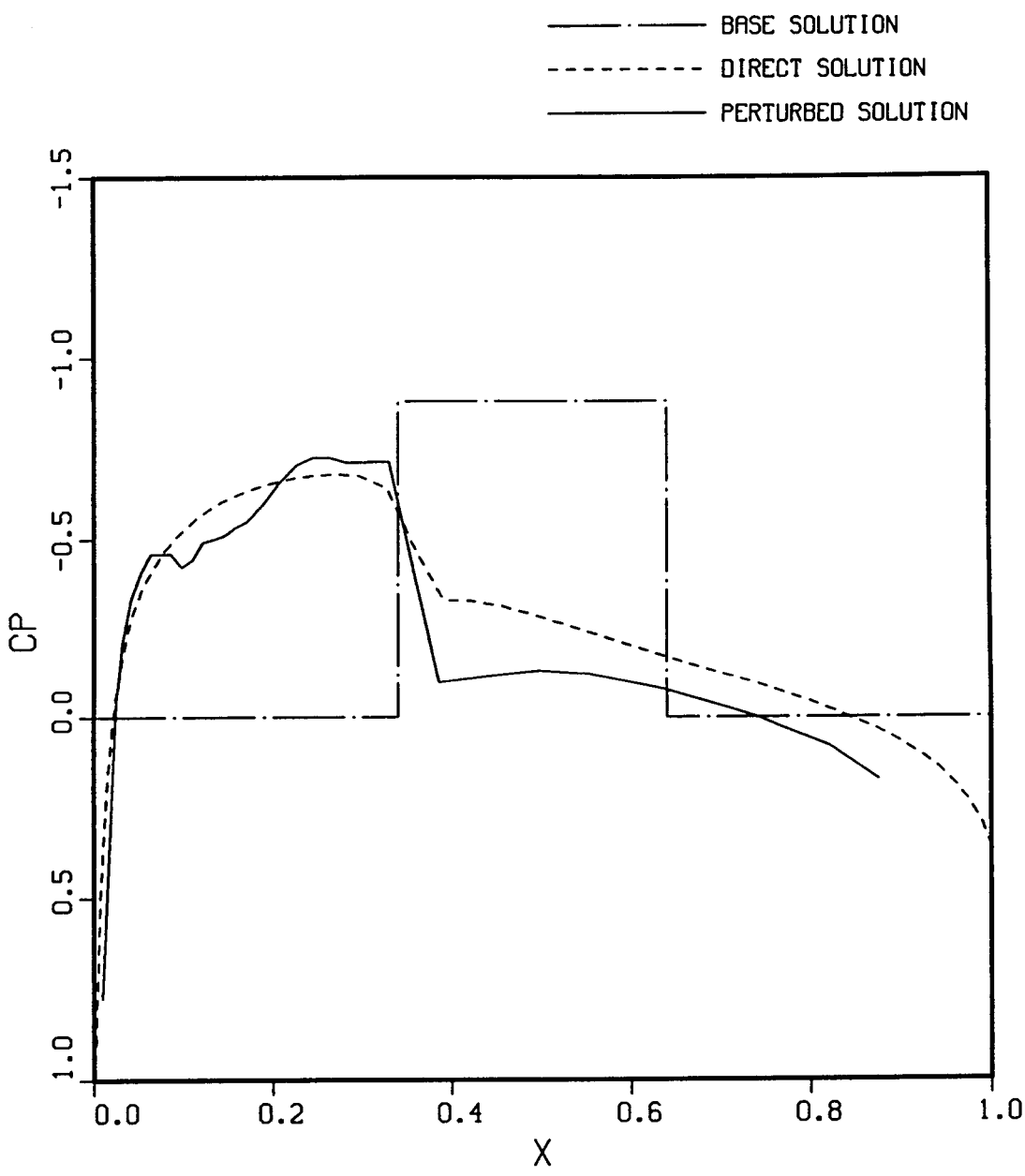

Figure 15.- Solution of Linear Constant Coefficient Equation with Modified Straining Terms (NACA 0010 Airfoil).

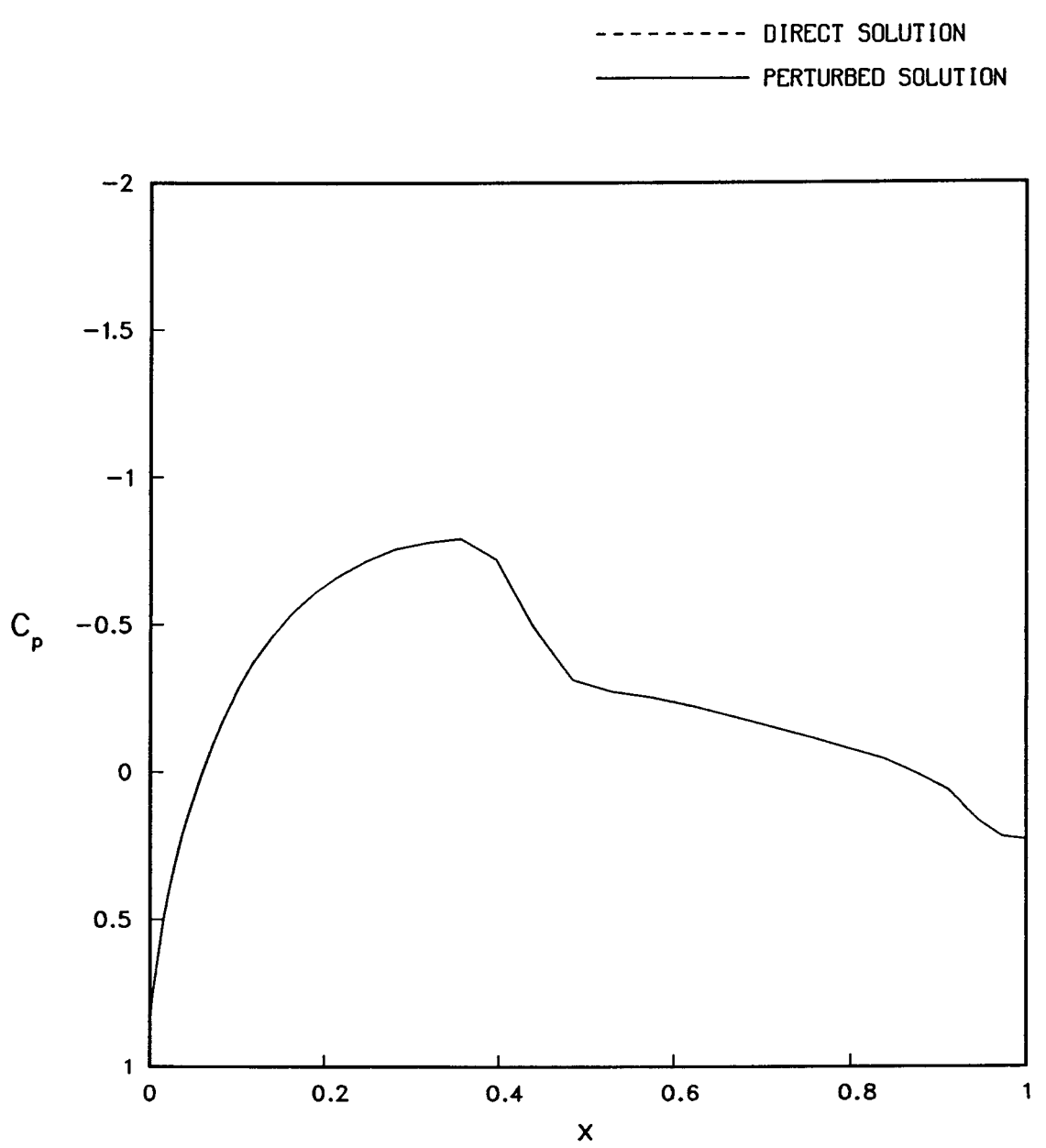

Figure 16.- Base Solution for Euler Equations (NACA 0010 Airfoil).

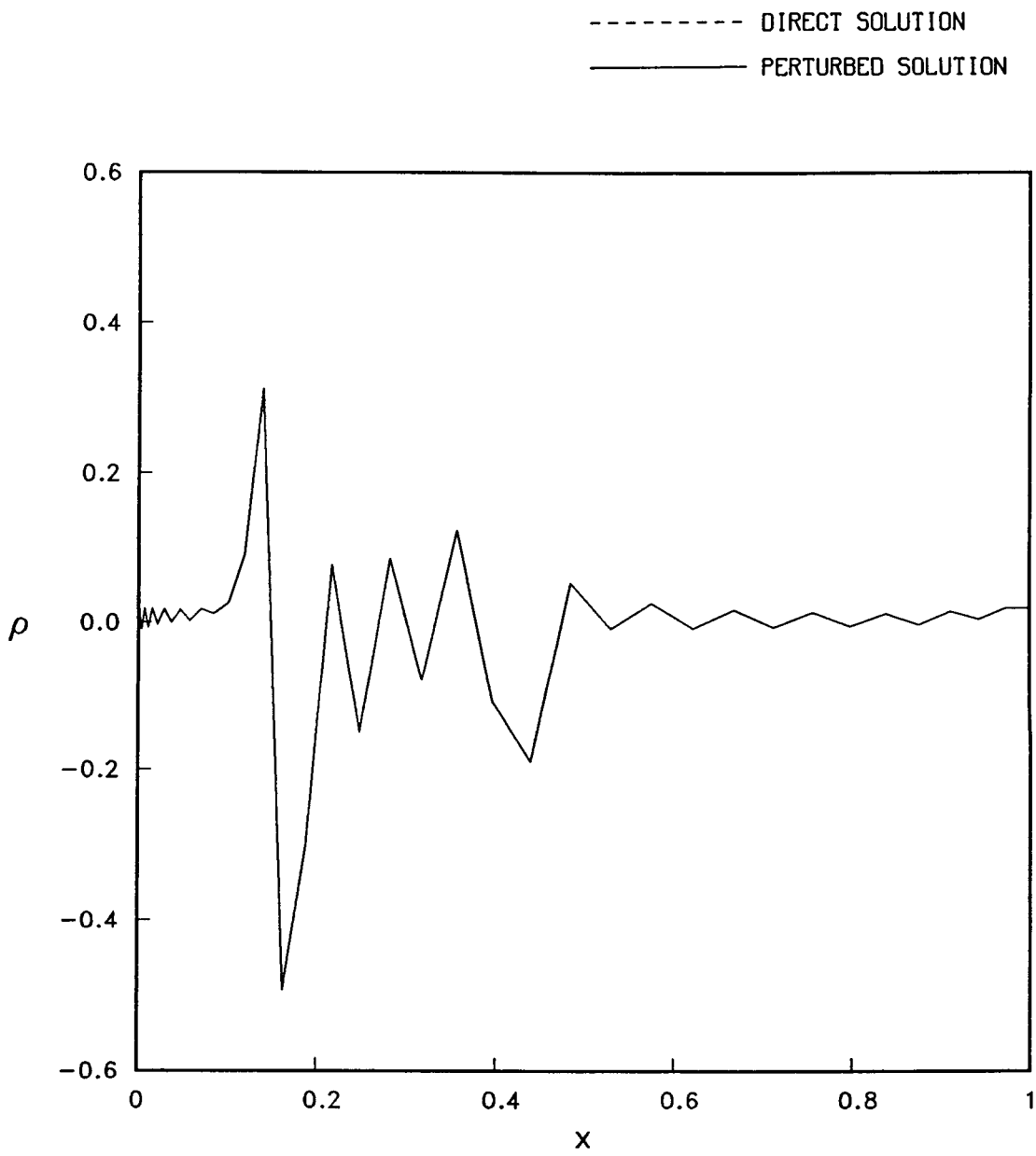

Figure 17.- Solution of Linear Euler Equation by Central Differences (NACA 0010 Airfoil).

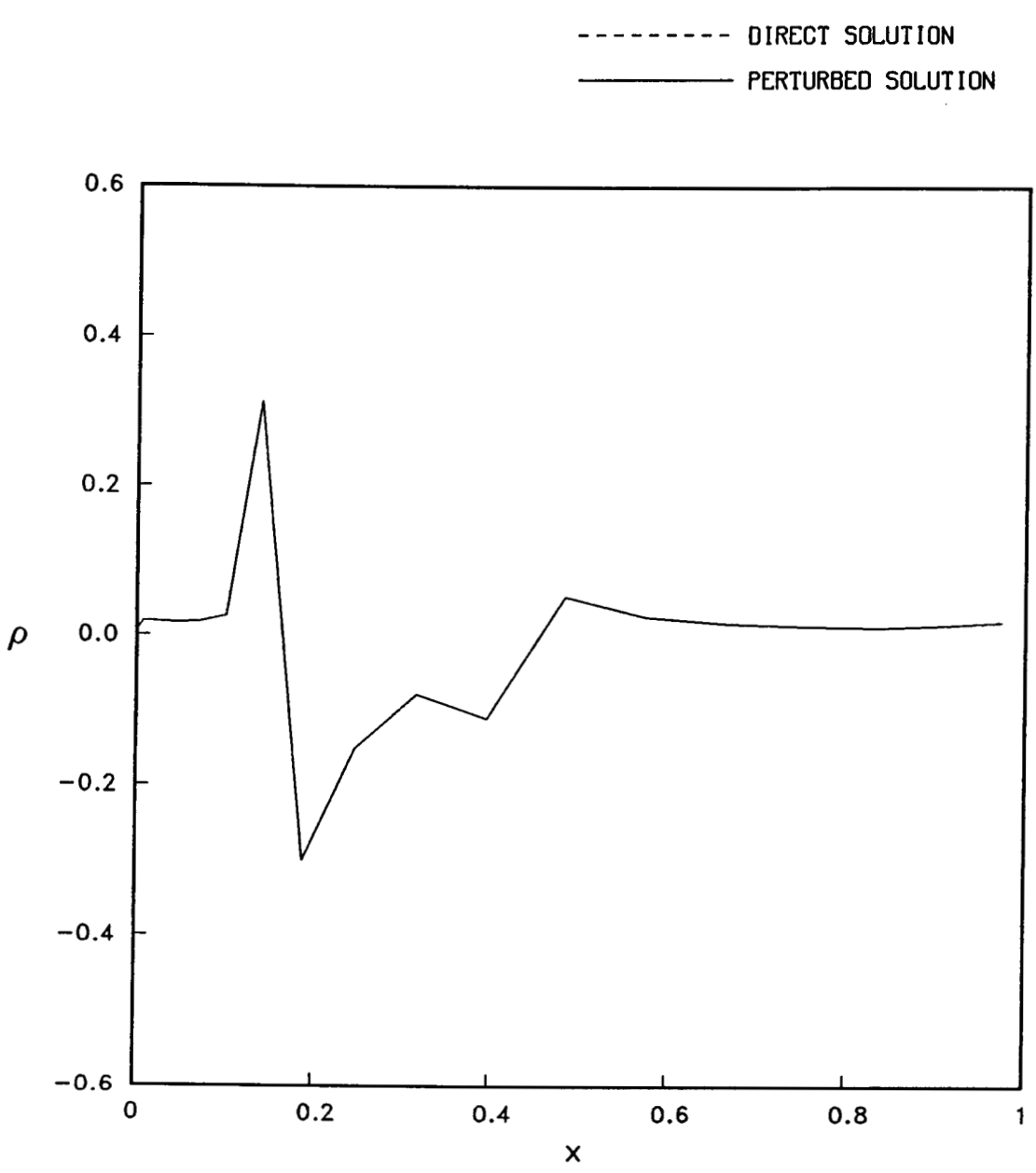

(a) Odd Points

Figure 18.- Solution of Linear Euler Equations by Central Differences with no straining.

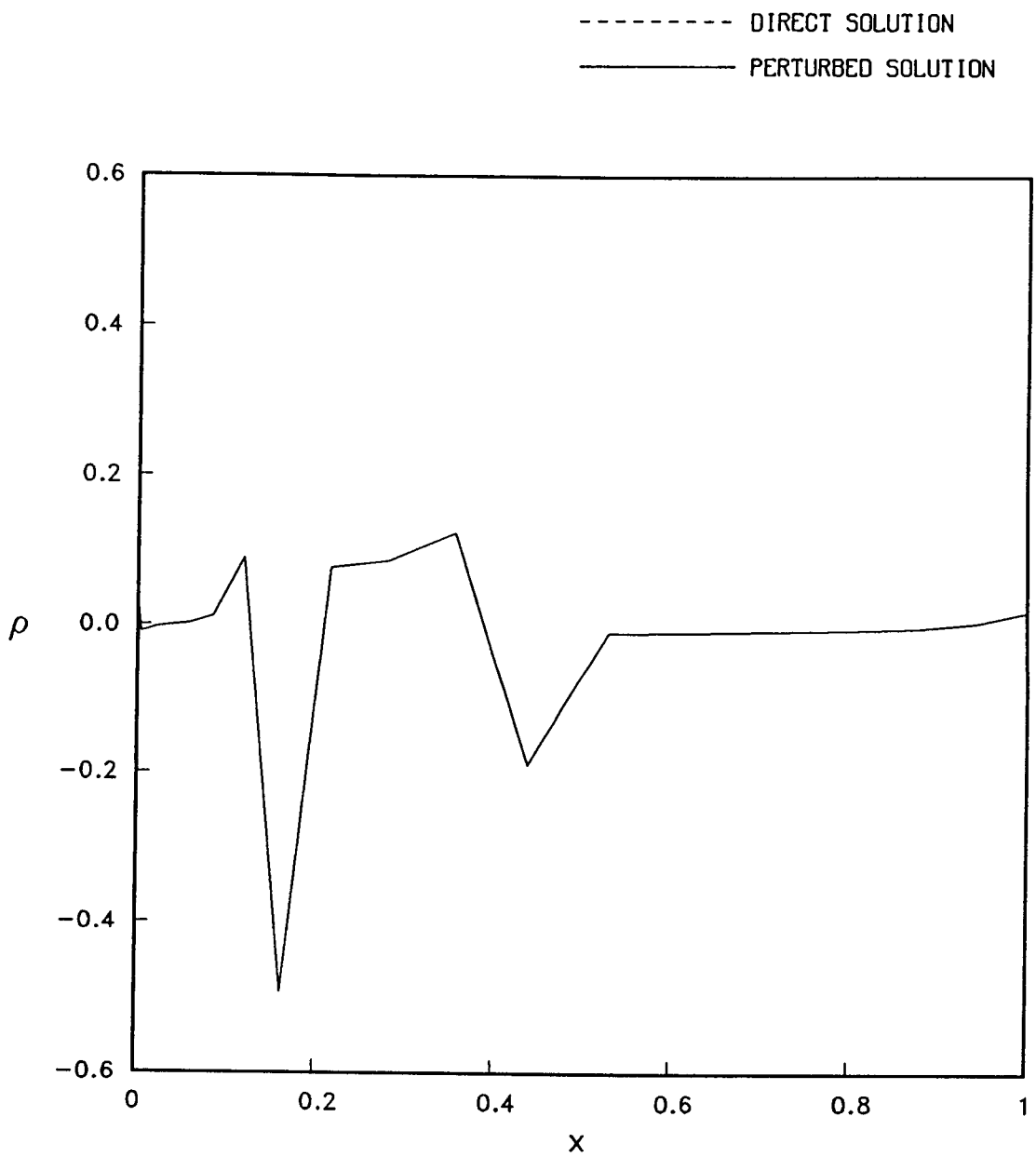

(b) Even Points.

Figure 18.- Concluded.

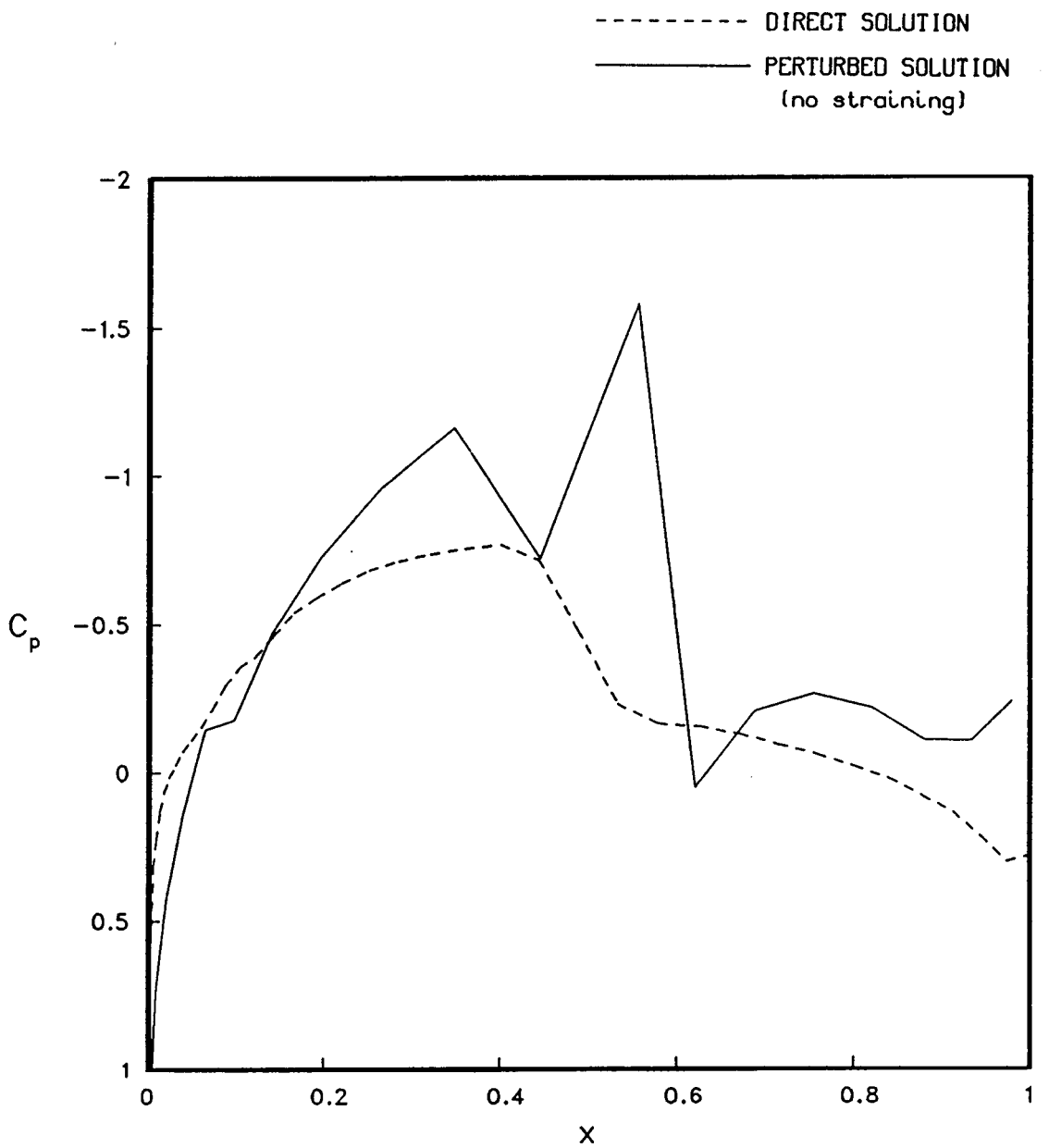

(a) Odd Points

Figure 19.- Solution of Linear Euler Equations with Coordinate Straining (NACA 0010 Airfoil).

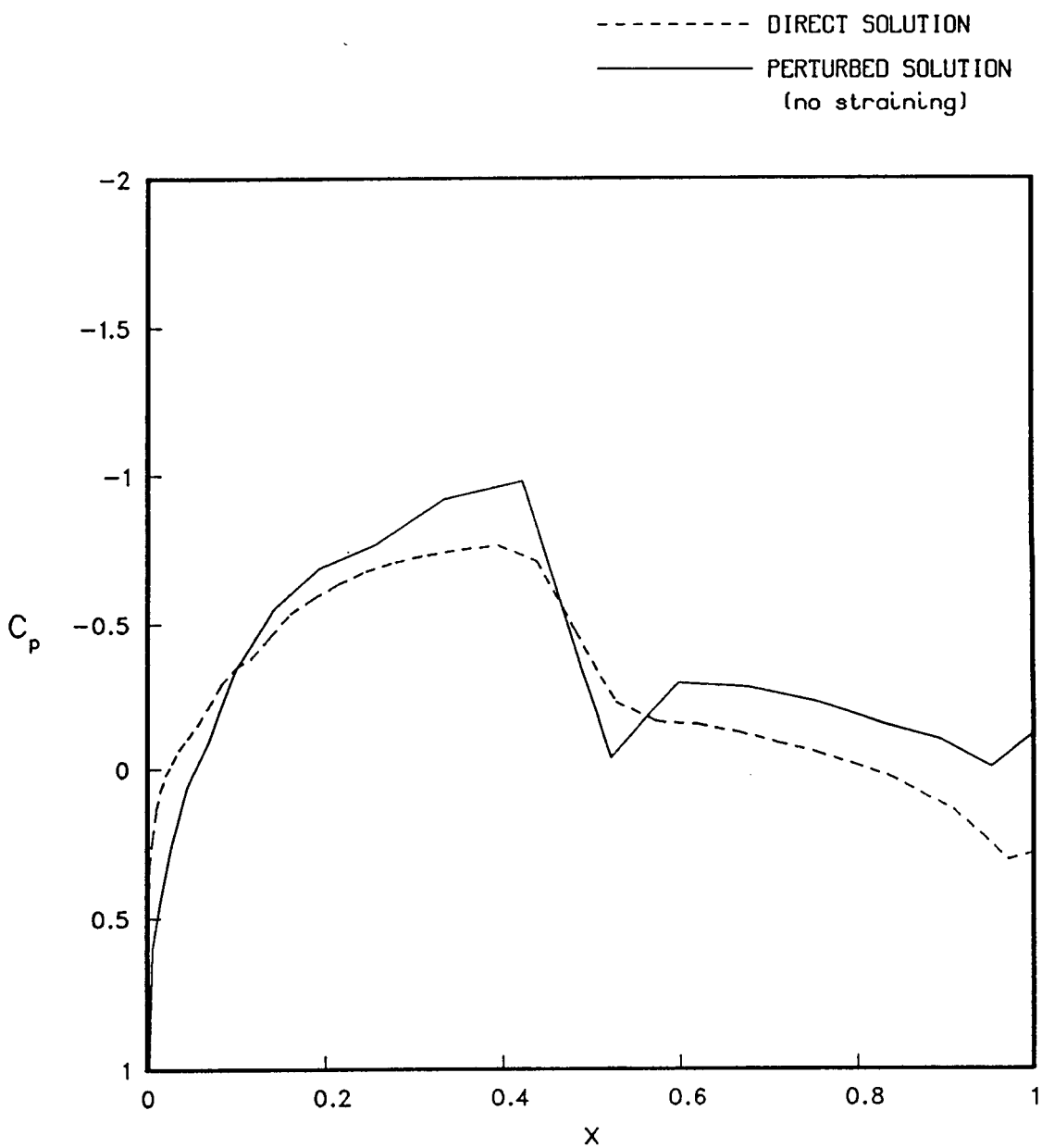

(b) Even Points

Figure 19.- Concluded.

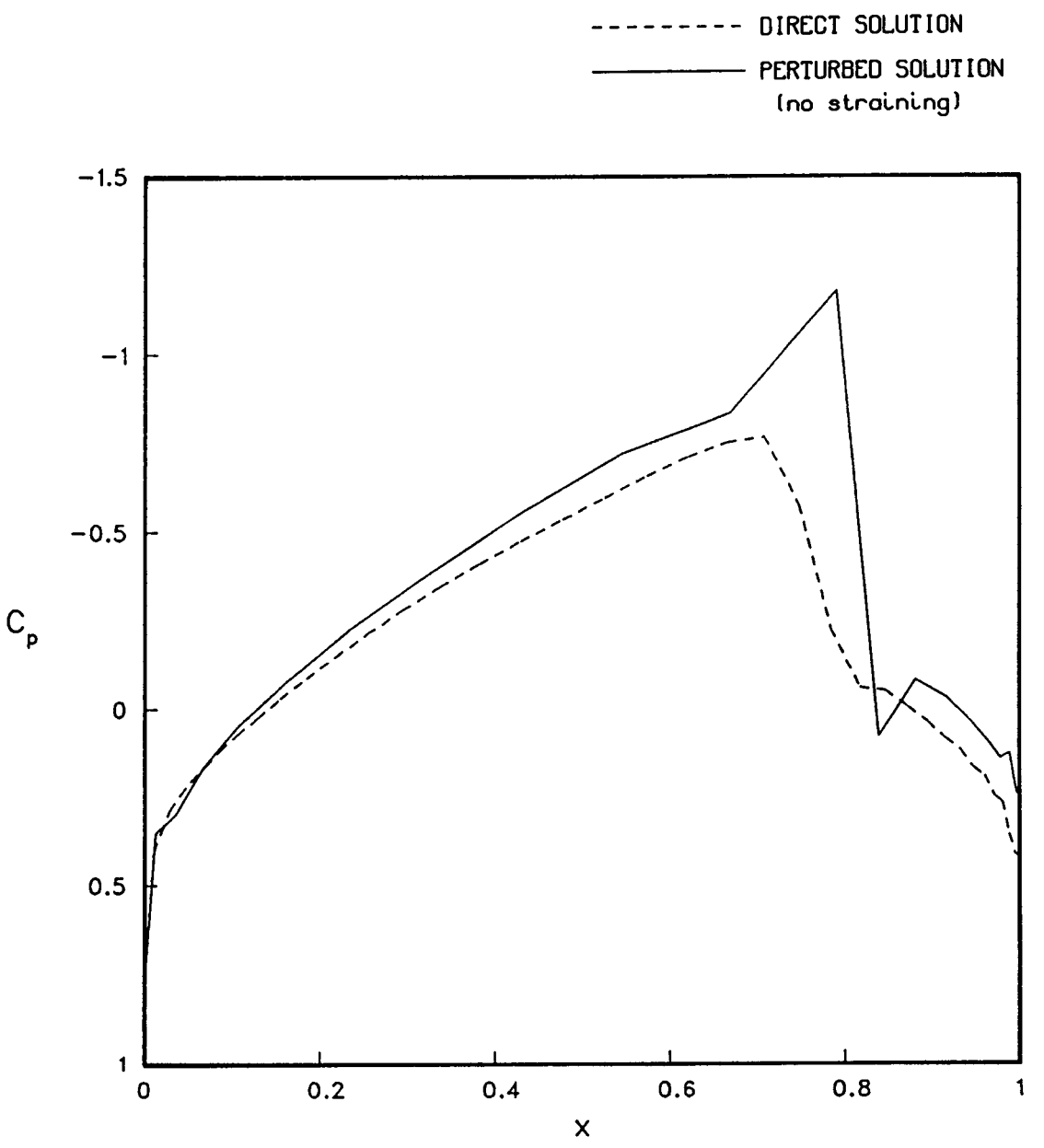

(a) Odd Points

Figure 20.- Solution for an 11% Biconvex Airfoil.

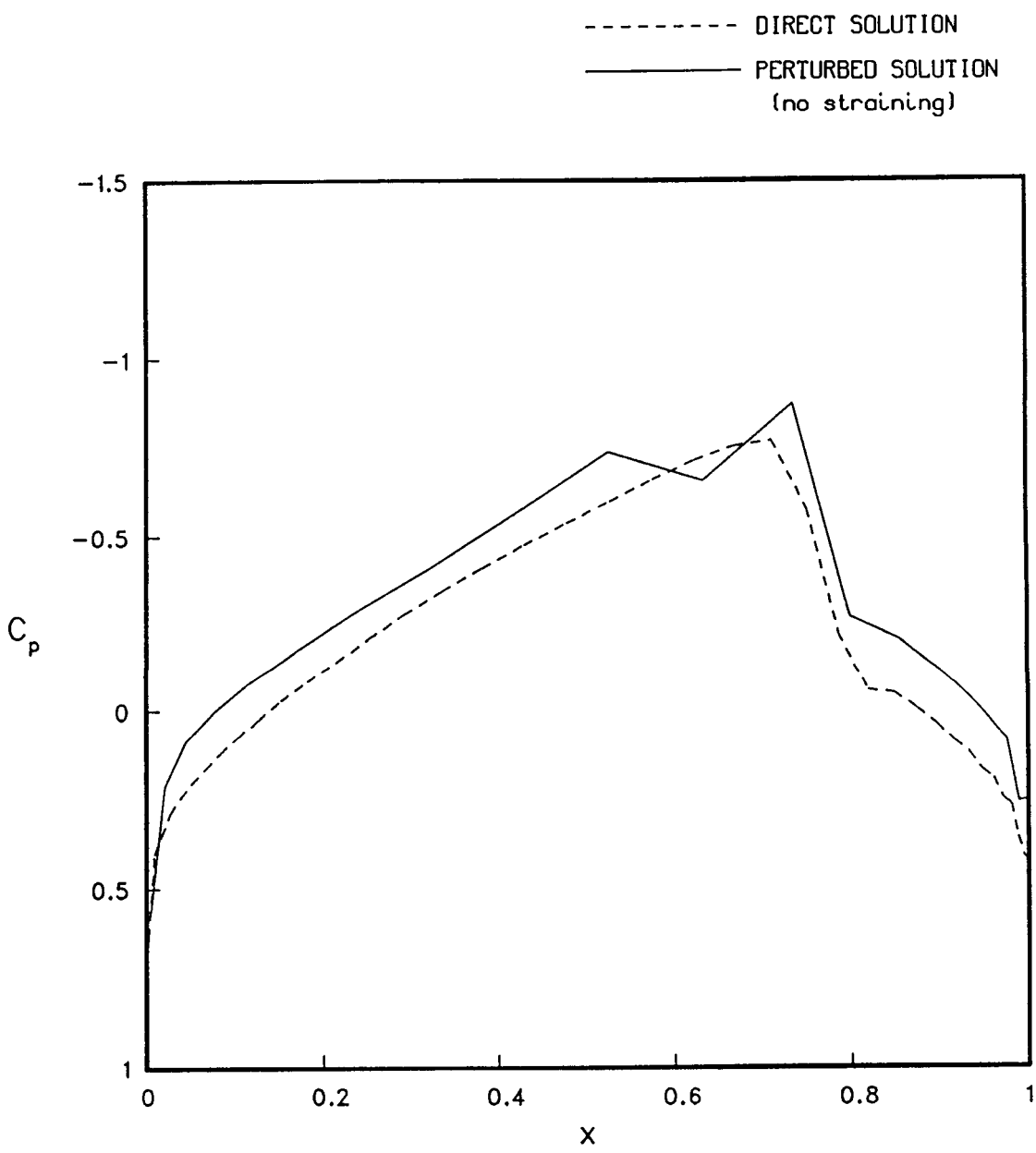

(b) Even Points

Figure 20b.- Concluded.